Treball de Fi de Grau

Grau en Enginyeria en Tecnologies Industrials

Study of the fluid effects on a submerged circular plate

REPORT

Author: Ainara Duran Hervás
Director: Francesc Xavier Escaler Puigoriol

Summons: September 2020

Escola Tècnica Superior
d'Enginyeria Industrial de Barcelona

Abstract

In this study, numerical analyses were performed to determine the effects of water loading and fluid-structure interactions on the axisymmetric modes of vibration of a free circular Chladni plate. A coupled structural-acoustic finite element model was built to study the modal properties of the circular plate. With structural modal and modal acoustic analyses, the axisymmetric natural frequencies and the mode shapes were determined for the plate in vacuum, in air and fully submerged in water. Numerical results were validated with theoretical results computed for the model plate. A better agreement was obtained in the vacuum and air cases, compared to the water results. The natural frequencies were seen to reduce due to the added mass effects of water, with an average frequency reduction ratio of 66,7%. On another hand, the mode shapes in water were also observed to change and differences between dry and wet modes were measured with the radii calculation of the nodal circles. Then, the effect of a solid boundary proximity on the axisymmetric modes was studied for the plate submerged in water. At different distances between the plate and the bottom wall, the natural frequencies were determined for the first 4 axisymmetric modes. A clear frequency reduction was observed as the wall got near to the plate. Variations within the different axisymmetric modes were quantified computing the frequency ratios for every relative wall distance. Finally, two-way coupled Fluid-Structure Interaction (FSI) transient simulations were performed for the Chladni circular plate in water. The interactions between the fluid and the plate were studied when the plate is fixed at its centre.

Summary

1. GLOSSARY ____ 7

2. PREFACE ____ 9

2.1. Project's origins and motivation 9

3. INTRODUCTION ____ 11

3.1. Objectives 12

3.2. Scope 12

4. BACKGROUND ____ 14

4.1. Mode shapes of vibration of a free circular plate 14

4.2. Axisymmetric vibrations of a completely free circular plate 15

4.3. FSI Governing equations 17

5. MECHANICAL MODEL ____ 19

5.1. Plate's properties 19

5.2. Model validation 20

5.3. Design and mesh 21

6. MODAL ANALYSIS RESULTS ____ 25

7. WALL DISTANCE REDUCTION EFFECTS ____ 31

8. TWO-WAY COUPLED ANALYSIS ____ 36

8.1. Defining the Structural Analysis System 37

8.2. Defining the Fluid Flow (CFX) Analysis System 38

8.3. Defining the coupling in the System Coupling application 41

8.4. Solving the two-way coupled analysis 42

8.5. Two-way coupled analysis results 43

9. PLANNING ____ 53

10. BUDGET ____ 55

10.1. Personnel costs 55

10.2. Infrastructure costs 56

11. ENVIRONMENTAL IMPACT ____ 58

CONCLUSIONS ____ 59

BIBLIOGRAPHY ____ 60

References 60
Additional literature 61

1. Glossary

***Chladni plate**:* flat plate with a small central hole to be mounted on an electrodynamic shaker.

***Fluid-Structure Interaction (FSI)**:* Multiphysics study of how fluids and structures interact.

***Rayleigh-Ritz method**:* direct method to find an approximate solution for boundary value problems.

***Flexural Rigidity**:* measure of stiffness of a structure when subjected to bending.

***APDL**:* Ansys Parametric Design Language.

Modal analysis: Mechanical APDL model used to study the dynamic characteristics of a structure under vibrational excitation (frequency domain).

Two-way coupling: mutual interaction between a structure and a fluid where both are affected to each other.

2. Preface

2.1. Project's origins and motivation

This project comes from my interest in Mechanics and particularly in Fluid Mechanics, which arouse in my third year of Bachelor. I've always been quite curious, so maybe that's why I felt a special attraction to this investigation when it was presented to me. I was introduced to previous experimental and numerical investigations that had been done in the Fluid Mechanics Department of ETSEIB-UPC and I thought that it was a great opportunity to contribute in this particular area of study. For this reason, I decided to take in on the study of the axisymmetric vibrations of a circular plate in air and fully submerged in water.

Knowing what had been done, I understood what would be interesting to test and study, so I was excited to undertake new goals that hadn't yet been achieved. One of them would be the completion of coupled fluid-structure simulations, which could be a very attractive interdisciplinary tool to use in the future. In fluid-structure interaction problems, both Structures and Fluid Mechanics are implied, so the two engineering disciplines should be considered. The combination of the two of them may be more challenging, but it is certainly the modern point of view and the closest approach to deal with real situations.

Taking as a start the work carried out by Escaler and De La Torre on their paper *Axisymmetric vibrations of a circular Chladni plate in air and fully submerged in water* (2018)[1], this project implements numerical analyses to determine the effects of water loading on the axisymmetric modes of vibration on a completely free circular plate. Also, the action of a solid boundary that disturbs the fluid waves is studied and examined on the mode shapes and on the natural frequencies of the circular plate.

Furthermore, this project may be extended with future research and may be useful for other investigations. In order to understand how fluid and structures interact, the study of a simple structure system is basic and more applicable for special interests. On another hand, conclusions taken on the fluid's effects on vibrating structures can be important to take into account in many design situations.

3. Introduction

Since the past two decades, the fluid-structure interaction (FSI) phenomena has been intensely studied in different fields of Fluid Mechanics. Particularly in hydraulics, FSI problems are getting the centre of attention of many recent investigations as precise dynamic calculations are sought for pipelines and water turbines. In vibrational dynamic responses, modal properties of fully or partially submerged bodies have been commonly treated as in air, but from experimental and numerical investigations it's been seen that significant differences exist.

In this sense, Amabili et al. (1995)[2], Amabili et al. (1996)[3], Amabili (1996)[4] and Amabili and Kwak (1996)[5] introduced theoretical results of the natural frequencies and modes in free vibrations of circular and annular plates coupled with fluids. The Rayleigh-Ritz method was used to remove the simplifying hypothesis that dry and wet mode shapes are the same and differences were quantified using the mass added approach. Following these results, Escaler and De La Torre (2018)[1] experimented with a simple structure and quantified the modal differences between air and water with experimental results and numerical simulations. Natural frequencies and mode shapes of the axisymmetric vibrations of a circular plate were determined applying the Chladni technique, which allows the visualization of nodal lines of vibrating plates by sprinkling sand on them. The sand piles up at the nodes moving out from oscillating regions, and so modal patterns can be observed by exciting the plate at a specific frequency. The Chladni technique has been commonly used in air configurations, but in that case, it was additionally proved to work with fully submerged bodies in still water.

Moreover, many investigations go further and study possible boundary conditions effects. Not only different conditions applied to the structure can help to understand the fluid-structure interaction, but also the fluid's properties. In this sense, Askari et al. (2013)[6] investigated on the effects of liquid height, submerged depth and lateral gaps in the vibration of circular plates immersed in a liquid-filled container with free surface.

The present study comes from the interest in enlarging the knowledge of the fluid's behaviour when a general simple structure is vibrating. Numerical simulations will be used to study the circular plate case, introducing advanced FSI analyses that have not already been employed in the ETSEIB Mechanics Department.

3.1. Objectives

The aim of this project is to study the modal response of a plate fully submerged in a fluid and to analyse the effects of a solid boundary proximity. In order to understand the fluid's behaviour in submerged vibrating structures, advanced coupled simulations will be employed and introduced.

Concretely, the natural frequencies of the axisymmetric modes of vibration will be numerically determined for a circular Chladni plate completely free in vacuum, in air and fully submerged in water. In those modes, the wall condition effects will be studied and the change in the natural frequencies will be evaluated as a function of different solid-wall distances. Then, the objective is to use transient coupled simulations to provide a wider understanding of the fluid-structure interaction and its consequences on the plate's motion. The application of two-way coupled analyses in Fluid-Structure Interaction (FSI) problems is particularly attractive in the field, but in many cases it has not yet been implemented. Consequently, the introduction to this type of analyses is an emphasized ambition that, moreover, can be very interesting for current and future investigations.

3.2. Scope

The scope of this project comprises the understanding of the model built and the study of the plate's modal properties in vacuum, in air and fully submerged in water. Specifically, the first six axisymmetric modes of vibration of the circular plate will be studied using numerical analysis. To do so, structural modal and modal acoustic analyses will be performed to examine the modal behaviour of the plate in vacuum, in air and in water, separately. In the last two cases, the fluid's effects on the axisymmetric modes of the plate will be evaluated and compared.

In order to analyse the influence of a solid boundary proximity, the distance between the plate and the bottom boundary of the fluid acoustic body will be reduced. In a real case, this bottom boundary would relate to the rigid wall of a fluid container, so boundary conditions will be applied accordingly. Modal acoustic analyses will be implemented at different wall distances to determine the axisymmetric modes of the plate, particularly in water. Then, the effects of the wall proximity will be evaluated considering the differences between the different modes and at changing distances.

Then, two-way coupled FSI simulations will be performed to examine the fluid and the plate's behaviours in real time, as well as the interaction between them. The excitement at particular frequencies will be modelled, so that transient state simulations can be executed at the natural frequencies of the plate.

The results obtained relative to the axisymmetric modes of the circular plate will be contrasted with previous theoretical and experimental investigations. From those, the study will concrete on the particular model built, which considers future experimental validation. In this hypothetical real model, the plate would be harmonically excited at its centre through an extension bar leaving its outer edge totally free. The numerical model of this project is based on this real model and considers the available material to implement the experiment. For this reason, the dimensions and the material properties will keep the same as in the experimental model for the single plate. However, the bar will be suppressed so as to simulate a completely free circular plate.

Finally, all the numerical simulations and analyses will be computed with the Student version of the software Ansys, which is limited to a maximum of 32000 nodes in the Structural physics and of 512000 nodes in the Fluid physics.

4. Background

4.1. Mode shapes of vibration of a free circular plate

The modes of vibration of a circular plate refer to the patterns of motion described by the structure when excited sinusoidally at a specific frequency. The normal modes are associated with standing wave patterns, which describe peak amplitude oscillations that are constant in time. Then, for a free circular plate excited by its centre, maximum transverse deformation occurs at the frequencies of the normal modes, known as the natural frequencies.

In the case of circular plates, mode shapes are characterized by nodal diametric lines and nodal concentric circles. For a completely free circular plate in vacuum, the first six mode shapes are shown in Figure 1, where n is the number of nodal diameters and s is the number of nodal concentric circles.

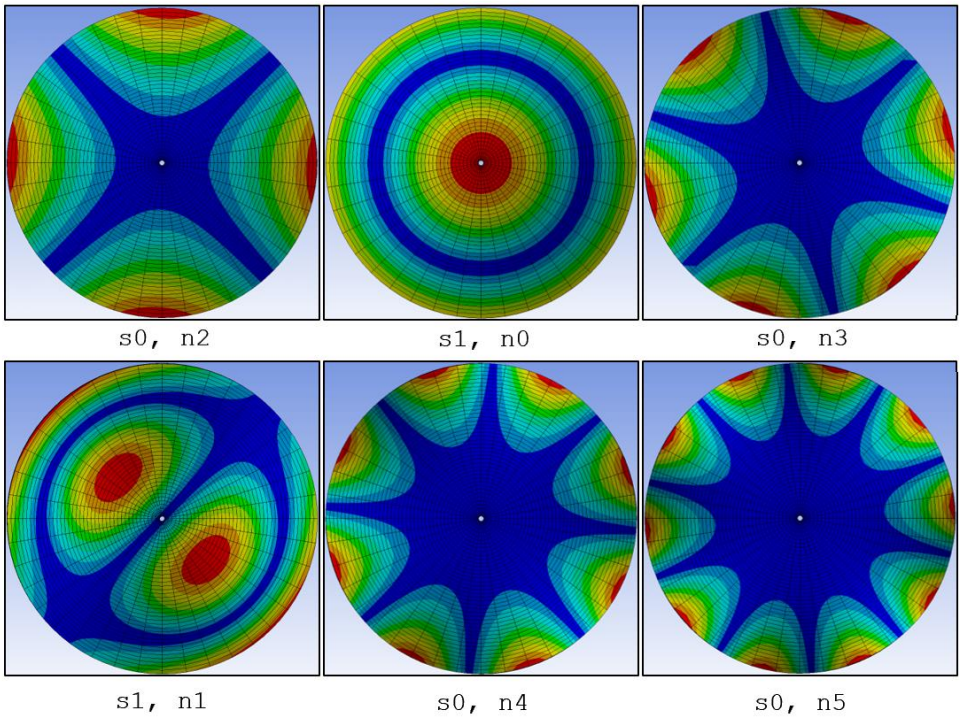

Figure 1. Mode shapes of a completely free circular plate in vacuum

This study focuses on the axisymmetric modes, that is, modes with no nodal diameter lines i.e. $n = 0$.

4.2. Axisymmetric vibrations of a completely free circular plate

Leissa (1969)[7] carried out a set of available results for the frequencies and mode shapes of free vibration of plates for design and development engineers. Experimental and theoretical results were provided for completely free circular plates by solving the classical differential equation of motion for the transverse displacement of a plate, given by

$$D\nabla^4 w + \rho_A \frac{\partial^2 w}{\partial t} = 0 \tag{1}$$

where D is the flexural rigidity defined by

$$D = \frac{Eh^3}{12\,(1-\nu^2)} \tag{2}$$

and E is the Young's modulus, h is the plate thickness, ν is the Poisson's ratio, ρ_A is the area density of the plate, t is time and $\nabla^4 = \nabla^2\nabla^2$, where ∇^2 is the Laplace operator.

Assuming free vibrations, the motion can be expressed as

$$w = W\cos\omega t \tag{3}$$

where ω is the angular frequency and W is a function of the position coordinates.

Substituting equations (3) into (1) yields

$$(\nabla^4 - \mathrm{k}^4)\,W = 0 \tag{4}$$

where k is defined as

$$\mathrm{k}^4 = \frac{\rho_A\omega^2}{D}. \tag{5}$$

For a solid circular plate with no internal holes and taking the origin of the polar coordinate system in the centre of the plate, the general solution to equation (4) becomes

$$W_n = [A_n J_n(kr) + C_n I_n(kr)]\cos n\theta \tag{6}$$

where n corresponds to the number of nodal diameters taking values from 0 to ∞, A_n and C_n are coefficients that determine the mode shape, J_n is a Bessel function of the first kind, I_n is a modified Bessel function of the first kind, r is the radius and θ is the polar angle.

Leissa (1969)[7] reported the natural frequencies of a completely free circular plate in terms of the roots λ^2, which are solutions to equation (6) and are defined as

$$\lambda^2 = wa^2\sqrt{\rho_A/D} \tag{7}$$

where a is the radius of the circular plate. For axisymmetric vibrations i.e. $n = 0$ and from $s1$ to $s6$ referring to the number of concentric circles from 1 to 6, results are indicated in Table 1 for $\nu = 1/3$.

From $s1$ to $s2$, Leissa (1969)[7] computed the relative radii r/a of the concentric nodal circles and determined it experimentally until $s6$. Presented as in Escaler and De La Torre (2018)[1], Table 2 shows the average of Leissa's theoretical and experimental results from $s1$ to $s5$, whereas only experimentally obtained are shown for $s6$.

Mode	s1	s2	s3	s4	s5	s6
λ^2	9,1	38,6	87,8	157,0	245,9	354,6

Table 1. Values of λ^2 for axisymmetric vibrations of a circular plate completely free and $\nu = 1/3$ from Leissa (1969)[7]

	r/a					
s1	0,680					
s2	0,843	0,391				
s3	0,895	0,591	0,257			
s4	0,918	0,692	0,441	0,190		
s5	0,956	0,753	0,548	0,351	0,154	
s6	0,958	0,794	0,624	0,456	0,292	0,131

Table 2. Relative radii r/a of nodal circles for axisymmetric vibrations of a circular plate in vacuum completely free and $\nu = 1/3$ from Leissa (1969)[7]

Kwak and Kim (1991)[8] introduced an analytical approach to estimate the effect of fluid on the natural frequencies of circular plates vibrating axisymmetrically in contact with fluid. They expressed the ratio between the natural frequencies in fluid and in air as a function of the added virtual mass incremental (AVMI) factor, which reflects the increase of inertia due to the presence of fluid. The AVMI factor β is defined as

$$\beta = \Gamma\left(\rho_f/\rho_p\right)(a/h) \tag{8}$$

where ρ_f is the fluid density, ρ_p is the plate density, a is the plate radius, h is the plate thickness and Γ is the non-dimensional added mass incremental (NAVMI) factor. Kwak (1991)[9] computed the NAVMI factor for a plate in contact with water on one side and for a plate in air – those results are shown in Table 3 as in Escaler and De La Torre (2018)[1].

For a plate completely immersed in water, the NAVMI factor must be doubled and the natural frequencies are obtained using the expression

$$f_{fluid} = \frac{f_{vacuum}}{\sqrt{1+\beta}} \tag{9}$$

where f_{fluid} and f_{vacuum} are the natural frequencies of the plate completely immersed in fluid and in vacuum, respectively.

	s1	s2	s3	s4	s5	s6
Γ	0,218247	0,137003	0,0962644	0,07401	0,06008	0,05056

Table 3. NAVMI factors for axisymmetric vibrations of a free circular plate and $\nu = 1/3$ with fluid on one side from Kwak (1991)[9]

4.3. FSI Governing equations

The governing equations in acoustic fluid-structural interaction (FSI) problems combine the structural dynamics equations with the Navier-Stokes (NS) mass and momentum conservation equations.

In order to obtain the acoustic wave equation, the NS equations are simplified by making the following assumptions: the fluid is compressible – density changes due to pressure variations, there is no mean flow of the fluid and pressure fluctuations are small compared to the mean pressure. Applying those assumptions and considering viscous dissipation, the following acoustic wave equation is obtained:

$$\nabla\left(\frac{1}{\rho_0}\nabla p\right) - \frac{1}{\rho_0 c^2}\frac{\partial^2 p}{\partial t^2} + \nabla\left[\frac{4\mu}{3\rho_0}\nabla\left(\frac{1}{\rho_0 c^2}p\right)\right] = -j\omega\left(\frac{Q}{\rho_0}\right) + \nabla\left[\frac{4\mu}{3\rho_0}\nabla\left(\frac{Q}{\rho_0}\right)\right] \tag{10}$$

where c is the speed of sound in the fluid medium defined by

$$c = \sqrt{\frac{K}{\rho_0}} \tag{11}$$

and K is the bulk modulus of the fluid, ρ_0 is the mean fluid density, μ is the dynamic viscosity, p is the acoustic pressure, t is time, Q is the mass source in the continuity equation and ω is the acoustic pressure angular frequency.

For a harmonically varying pressure, equation (10) becomes:

$$\nabla\left(\frac{1}{\rho_0}\nabla p\right) - \frac{\omega^2}{\rho_0 c^2}p + \nabla\left[\frac{4\mu}{3\rho_0}\nabla\left(\frac{1}{\rho_0 c^2}p\right)\right] = -j\omega\left(\frac{Q}{\rho_0}\right) + \nabla\left[\frac{4\mu}{3\rho_0}\nabla\left(\frac{Q}{\rho_0}\right)\right] \tag{12}$$

where p is the acoustic pressure amplitude.

The finite element formulation is obtained from discretization, conducing to the following expression in matrix notation:

$$\boldsymbol{M_F}\ddot{\boldsymbol{p}}_{\boldsymbol{e}} + \boldsymbol{C_F}\dot{\boldsymbol{p}}_{\boldsymbol{e}} + \boldsymbol{K_F}\boldsymbol{p}_{\boldsymbol{e}} + \overline{\rho_0}\boldsymbol{R}^T\ddot{\boldsymbol{u}}_{\boldsymbol{e,F}} = \boldsymbol{f_F} \tag{13}$$

where $\boldsymbol{M_F}$ is the acoustic fluid mass matrix, $\boldsymbol{p_e}$ is the nodal acoustic pressure vector, $\boldsymbol{C_F}$ is the acoustic fluid damping matrix, $\boldsymbol{K_F}$ is the acoustic stiffness matrix, $\boldsymbol{R}$ is the acoustic fluid boundary matrix, $\overline{\rho_0}$ is the acoustic fluid mass density (constant), $\boldsymbol{u_{e,F}}$ is the nodal displacement vector and $\boldsymbol{f_F}$ is the acoustic fluid load vector.

Finally, the program resolves the combination of acoustic and structural matrices. For time-dependent analysis (transient), it is known as the unsymmetrical coupled FSI matrix system

$$\begin{bmatrix} \boldsymbol{M_S} & 0 \\ \overline{\rho_0}\boldsymbol{R}^T & \boldsymbol{M_F} \end{bmatrix}\begin{Bmatrix} \ddot{\boldsymbol{u}}_{\boldsymbol{e}} \\ \ddot{\boldsymbol{p}}_{\boldsymbol{e}} \end{Bmatrix} + \begin{bmatrix} \boldsymbol{C_S} & 0 \\ 0 & \boldsymbol{C_F} \end{bmatrix}\begin{Bmatrix} \dot{\boldsymbol{u}}_{\boldsymbol{e}} \\ \dot{\boldsymbol{p}}_{\boldsymbol{e}} \end{Bmatrix} + \begin{bmatrix} \boldsymbol{K_S} & -\boldsymbol{R} \\ 0 & \boldsymbol{K_F} \end{bmatrix}\begin{Bmatrix} \boldsymbol{u}_{\boldsymbol{e}} \\ \boldsymbol{p}_{\boldsymbol{e}} \end{Bmatrix} = \begin{Bmatrix} \boldsymbol{f_S} \\ \boldsymbol{f_F} \end{Bmatrix} \tag{14}$$

where $\boldsymbol{f_S}$ is the structure load vector and $\boldsymbol{M_S}$, $\boldsymbol{C_S}$ and $\boldsymbol{K_S}$ are the structure solid mass, the damping and the stiffness matrices, respectively.

For steady state simulations, that is, in modal acoustic analysis, structural and acoustic modes are coupled following the equation:

$$\left(-\omega^2\begin{bmatrix} \boldsymbol{M_S} & 0 \\ \overline{\rho_0}\boldsymbol{R}^T & \boldsymbol{M_F} \end{bmatrix} + j\omega\begin{bmatrix} \boldsymbol{C_S} & 0 \\ 0 & \boldsymbol{C_F} \end{bmatrix} + \begin{bmatrix} \boldsymbol{K_S} & -\boldsymbol{R} \\ 0 & \boldsymbol{K_F} \end{bmatrix}\right)\begin{Bmatrix} \boldsymbol{u}_{\boldsymbol{e}} \\ \boldsymbol{p}_{\boldsymbol{e}} \end{Bmatrix} = 0 \tag{15}$$

5. Mechanical model

5.1. Plate's properties

The model of circular plate was taken from a real plate available in the Fluid Mechanics Laboratory in ETSEIB-UPC. The reason to choose that one was to open up the possibility of continuing this investigation and validate the numerical results with experimental evidences. Indeed, the Chladni plate used in Escaler and De La Torre (2018)[1] was this same one.

The circular plate had an outer radius a of 0,12 m and a thickness h of $0{,}8 \cdot 10^{-3}$ m. In practice, the plate was thought to be harmonically excited by its centre with a support bar connected to a frequency electrodynamic shaker. For those clamping purposes, the plate had an inner small hole of $4 \cdot 10^{-3}$ m. The material of the plate was T6 temper 6061 aluminium alloy with a density ρ_p of 2700 kg/m^3, a Young modulus E of 69 GPa and a Poisson ratio ν of 0,35. For this plate, the flexural rigidity D was of 3,355 Nm.

The fluids tested would be air and still water, whose mechanical properties are resumed with the plate's ones in Table 4. The fluids' domain was chosen in accordance with the dimensions of a tank cavity from the laboratory, which had already been used for similar purposes. The inner dimensions of the square tank were $0{,}48 \times 0{,}48 \times 0{,}49$ m^3 and an indication was marked in the 370 mm height to measure the fluid's volume. Consequently, the fluids' domain was set of $0{,}48 \times 0{,}48 \times 0{,}37$ m^3, placing the plate at a 0,16 m distance from its upper face to the upper fluid limit. More details about the geometry of the model will be exposed in section 5.3.

Material	Density [kg/m3]	Sonic speed [m/s]	Young modulus [GPa]	Viscosity [Pa s]
Aluminium	2700	-	69	-
Air	1,225	346,25	-	$1{,}7894 \cdot 10^{-5}$
Water	998,2	1482,1	-	$1{,}003 \cdot 10^{-3}$

Table 4. Mechanical properties of T6 temper 6061 aluminium, air and water

5.2. Model validation

For validation purposes, the Chladni plate was treated as a free circular plate. Considering the central hole very small compared to the plate outer diameter, numerical results could be contrasted with data based on Leissa (1969)[7] and Kwak (1991)[9]. In particular, Leissa's formulation would be used in vacuum and calculations for air and water would be based on Kwak's considerations for fluids.

Rearranging equation (7) and substituting the radius a, the flexural rigidity D and the calculated area density $\rho_A = 2{,}16$ kg/m^2, the plate's modal frequencies could be expressed as a function of λ^2 for the vacuum particular case. In rad/s, that is

$$\omega = \frac{\lambda^2}{a^2\sqrt{\rho_A/D}} = 86{,}548\lambda^2 \tag{16}$$

Substituting λ^2 with Leissa's values previously presented in Table 1, theoretical frequencies for the first six axisymmetric modes in vacuum were obtained, as shown (in Hz) in Table 5. It was taken into account that data from Table 1 held a Poisson ratio of 0,33 instead of the plate's 0,35. However, as it will be seen further on, it didn't come to be a significant difference that affected the results.

For the air and water cases, the AVMI factor β was calculated for the first six axisymmetric modes applying equation (8) and substituting the density of the fluid ρ_f, the plate's density ρ_p, the radius a, the thickness h and the doubled NAVMI factor Γ, whose values were shown in Table 3. Then, frequencies in air and water were calculated using equation (9) and the vacuum frequencies previously found.

Table 5 resumes the frequency theoretical results for the vacuum, air and water cases.

	s1	s2	s3	s4	s5	s6
$f_{vacuum\ th}$ [Hz]	125,1	531,0	1209,4	2162,6	3387,2	4884,5
$f_{air\ th}$ [Hz]	123,3	526,1	1201,6	2151,8	3373,4	4867,7
$f_{water\ th}$ [Hz]	24,9	131,9	353,9	712,7	1223,5	1900,2

Table 5. Natural frequencies of the axisymmetric modes of vibration for a circular plate completely free. Theoretical values in vacuum based on Leissa (1969)[7] and in air and in water based on Kwak (1991)[9]

5.3. Design and mesh

The numerical simulations of this project were performed with Ansys Student 2020 R1, the Ansys Workbench-based bundle of Ansys Mechanical, Ansys CFD, Ansys Autodyn, Ansys SpaceClaim and Ansys DesignXplorer. In particular, SpaceClaim 3D modelling software was used to design the geometry of the model and Mechanical APDL (Ansys Parametric Design Language) and CFX (the Ansys Computational Fluid Dynamics software) solvers were applied to carry out the numerical analyses.

According to the properties from section 5.1, the geometry design was built with SpaceClaim, available in ANSYS Mechanical 2020 R1 (Student Version). The plate faces were split resulting in extra edges that further on were used for mesh control objectives, as seen from Figure 2. Similarly, for acoustic analysis, the fluid domain was split and separated into different bodies so as to be able to define axisymmetric meshing patterns. In total, 8 acoustic bodies assembled the acoustic cavity: the small central hole, the plate's contour until the limit walls, the upper and downer contours, the upper and downer annular cylinders (plate extensions) and the upper-hole and downer-hole cylinders. Next, all acoustic bodies were joined up using the "Share" tool, that connected the selected coincident topologies as shown in Figure 3 – purple lines identify the shared edges. Thus, all acoustic bodies were connected for Workbench calculations but yet the mesh of every single body could be done separately. In Figure 4, the specific dimensions of the model are indicated.

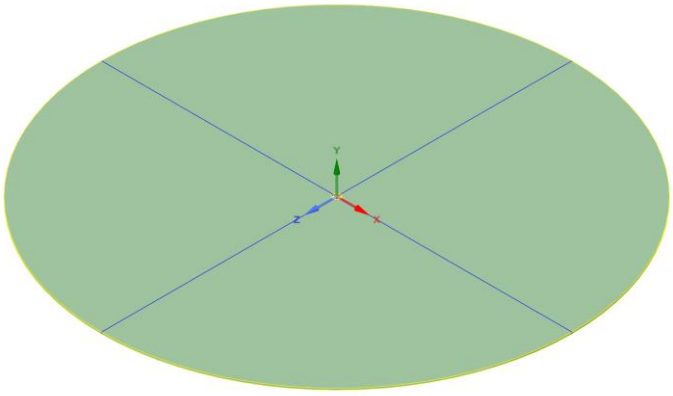

Figure 2. Model design of the circular plate

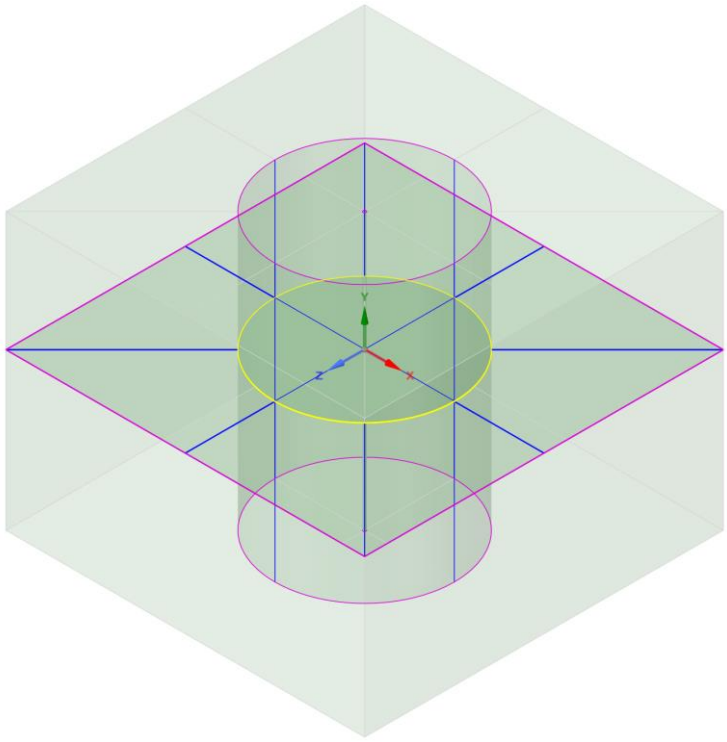

Figure 3. Model design of the total system (plate and acoustic separated bodies)

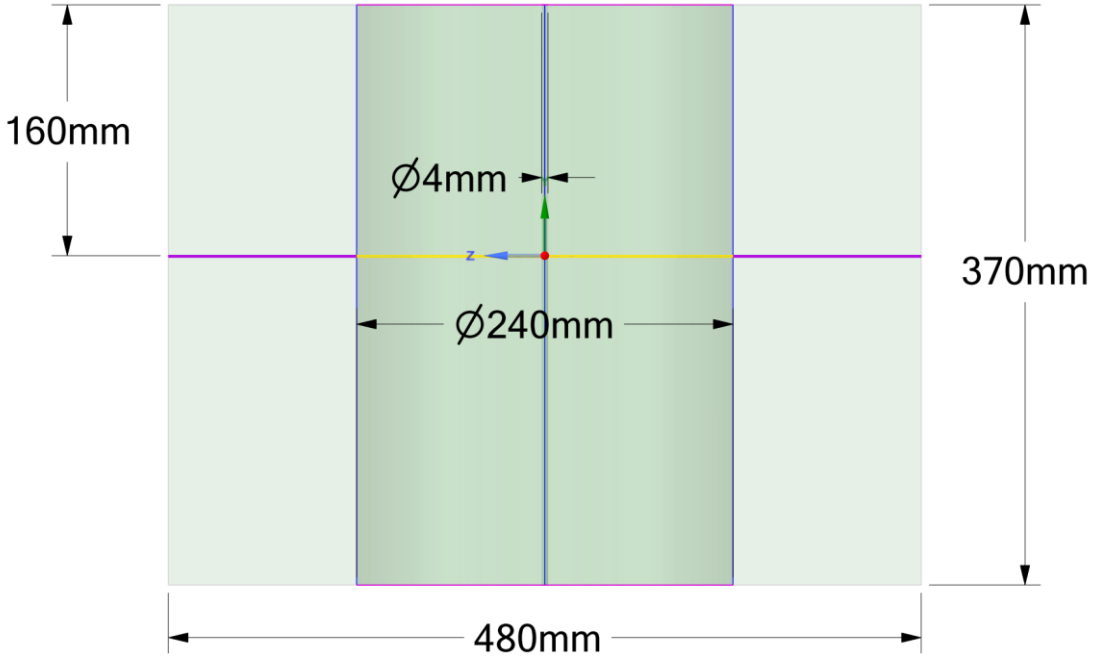

Figure 4. Model dimensions

Material properties were introduced in Engineering Data and subsequently assigned to each part of the geometry. Then, the mesh was carried out aiming the maximum high resolution considering the limits of the software license. As the number of nodes in the ANSYS Student version is constraint to 23000, the model was meshed with a total of 22133 nodes and 4960 elements. Despite the final mesh quality was below the optimum desired, the most important parts of the system were selected to have higher resolution. The strategy undertaken was to build a satisfactory mesh for the plate and follow the same pattern for the acoustic bodies with the highest possible resolution but still in the limits. For this reason, the plate and the elements near the plate were chosen to have smaller elements and so higher number of edge divisions.

The plate's mesh was designed with hexahedral elements using the "MultiZone" function. Considering the harmonic load to which the plate would be submitted later on, special emphasis was laid in the number of concentric circles, which was controlled with the sizing tool applied in the radial edges. The number of the perimeter divisions was also defined using the same tool in the bending edges. Figure 5 shows the plate mesh, with a total of 10 radial divisions and 40 perimeter divisions. More radial divisions would have been desired, but an equilibrium had to be reached with the fluid's mesh to stay in the limit of nodes.

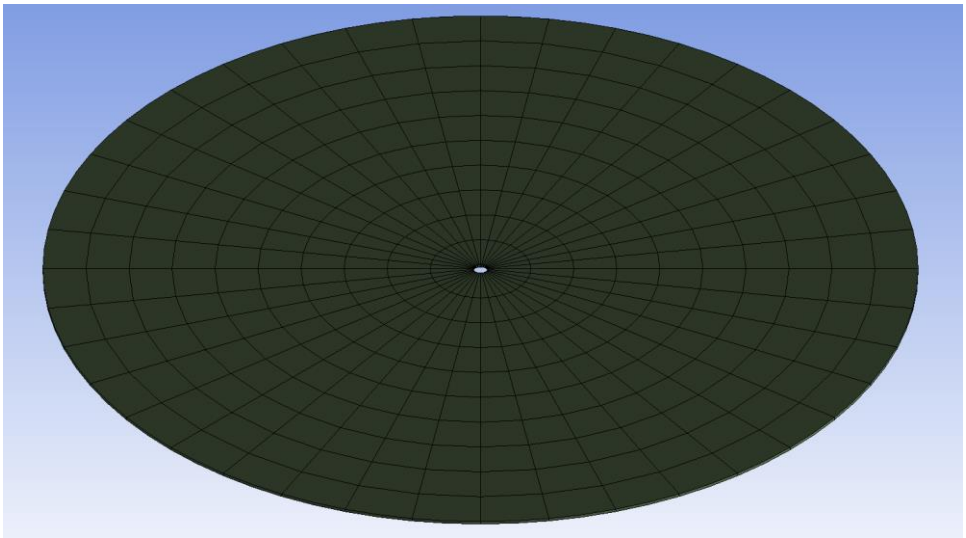

Figure 5. Plate mesh

The mesh of the acoustic bodies was built with lower mesh density, but following the same axisymmetric pattern. Again, it would have been suitable to have thinner elements in the surrounding area of the plate, but the limit of nodes was a significant constraint. Therefore, the decision made was to define the same mesh conditions in shared faces and softly reduce the size of the elements near the plate. This was introduced with the "bias" option

in the edge sizing tool. In the case of the contours radial edges, 3 divisions were set with a bias growth rate of 1,16 (smooth transition). For the longitudinal edges of the cylinders and contour bodies, 3 and 4 divisions were indicated in the upper and lower cases with a smooth bias growth rate of 1,3 and 1,2, respectively. The complete mesh of the system parts can be appreciated from Figure 6, which shows the sizing and the mesh pattern that was finally resolved.

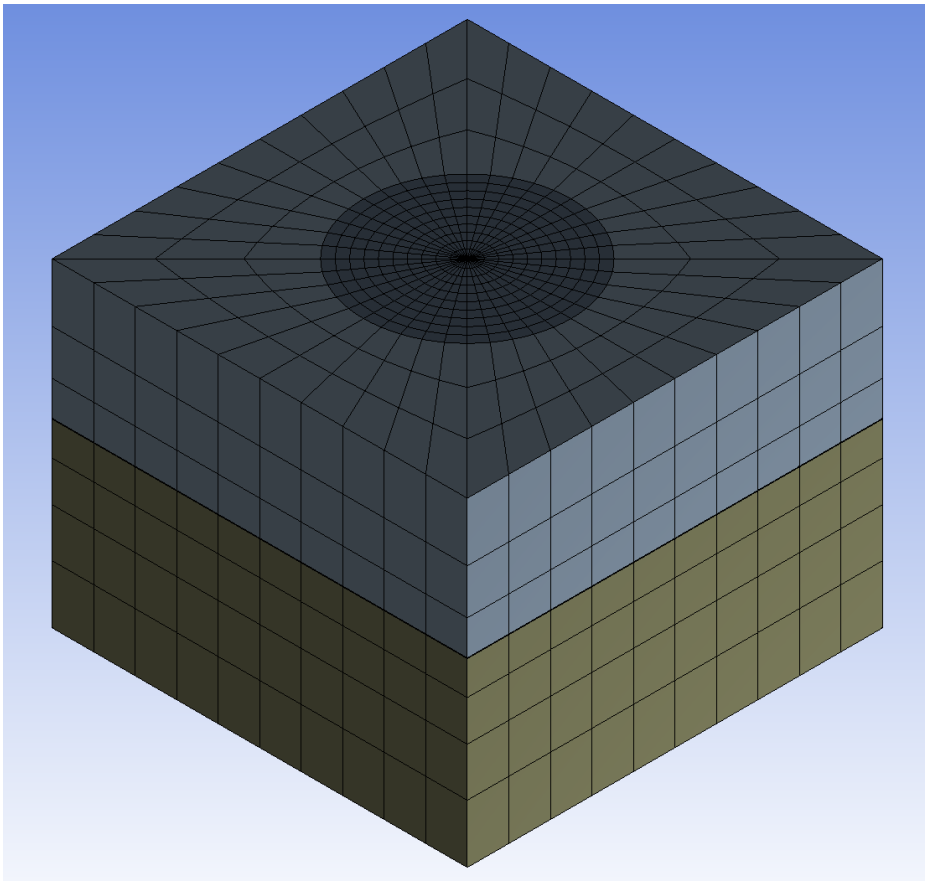

Figure 6. Mesh patterns of the acoustic bodies

6. Modal analysis results

Once completed the model design, modal analyses were carried out with Mechanical APDL (Ansys Parametric Design Language) solver. The plate's axisymmetric modes were studied in vacuum, in air and in water.

In the vacuum case, no fluid interacts with the structure, so the analysis is entirely structural. Consequently, no acoustic body must be present in the model and if so, it needs to be suppressed so that it is not taken into account. For this reason, only in this case it was possible to apply a more refined mesh of the structure. As the plate was decided to be studied totally free, no loads nor boundary conditions were applied. Then, frequency excitation was the only variable to control. In "Analysis Settings", the maximum number of modes to find can be specified, as well as the range of the frequency domain. When solved, all the modes that the solver has found within the frequency domain are displayed as frequency results. Applying the total deformation calculations for each mode, mode shape results can be created to visualize the animations of every frequency mode. Following these steps, the first six axisymmetric modes were found progressively changing the frequency range and observing the mode shape of each frequency.

Differently, in the air and water cases, fluid-structure interaction must be considered according to multiphysics problems. Therefore, modal acoustic analysis systems, which include acoustic settings and FSI analysis, were created for each case. For those analyses, the complete model (plate with fluid) was considered, so it was necessary to define each part. The 8 bodies conforming the acoustic cavity were defined as "Acoustic Region" whereas the plate was identified as "Physics Region". This way, only acoustic and structural properties would be applied in the fluid's and plate's parts, respectively. Then, the 16 shared common faces between the plate and the fluid were specified as "Fluid Solid Interface". In these faces, direct fluid-structure contact occurs and so it needs to be defined for FSI calculations. Finally, relative pressure of 0 Pa was applied in the upper wall of the fluid, as in the hypothetical real case this would be the only free contact wall. Once those boundary conditions were applied, mode shape results were displayed and the axisymmetric modes in air and water were explored as done in the vacuum case.

The found axisymmetric mode shapes of the plate in vacuum, in air and in water are shown in Figure 7, Figure 8 and Figure 9, respectively. In the vacuum case, the first six modes were easily determined, but for the air and water ones more difficulties were faced. The highest the frequencies, more problems seemed to appear in the acoustic modal system to find the modes. However, doing several trials with different increasing frequency ranges and changing the number of modes to find, the first 4 axisymmetric modes were found for water whereas only the first two were reached for air. For values higher than 1100 Hz, the solver was unable to find any modal mode.

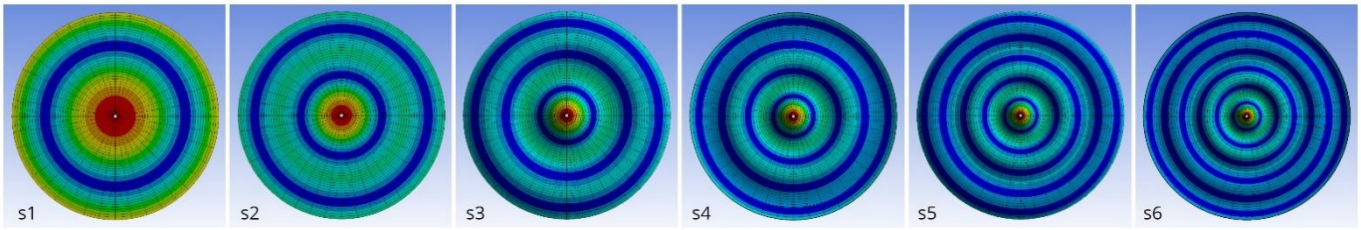

Figure 7. First 6 axisymmetric mode shapes of the circular plate in vacuuum

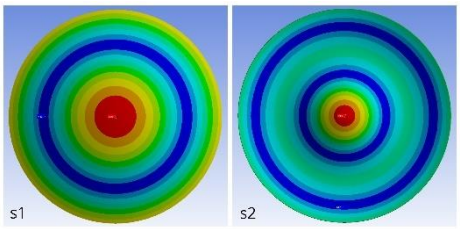

Figure 8. First 2 axisymmetric mode shapes of the circular plate in air

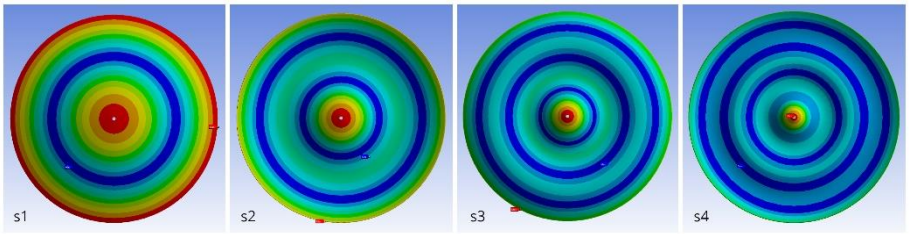

Figure 9. First 4 axisymmetric mode shapes of the circular plate in water

The frequency results are presented in Table 6 for each case, with the percent deviation relative to the theoretical values of Leissa (1969)[7] in the vacuum case and Kwak (1991)[9][9] in the air and water ones. Small differences with the theoretical values are deduced in the vacuum and air cases, as the highest percent deviation appears in the sixth mode of vacuum with a magnitude of 0,7%. On the contrary, important differences are observed in the water results, with higher deviations being 19,6% the highest in the first mode.

Mode	$f_{vacuum\ sim}$ [Hz]	dev [%]	$f_{air\ sim}$ [Hz]	dev [%]	$f_{water\ sim}$ [Hz]	dev [%]
s1	125,4	0,2	123,7	0,3	29,8	19,6
s2	530,1	-0,2	525,8	-0,06	151,7	14,9
s3	1206,9	-0,2	-		403,6	14,0
s4	2153,5	-0,4	-		822,8	15,4
s5	3368,9	-0,5	-		-	
s6	4852,0	-0,7	-		-	

Table 6. Simulated results of the natural frequencies of the axisymmetric modes of vibration for a circular plate completely free in vacuum, air and water. Percent deviations (dev) relative to the theoretical values exposed in Table 5.

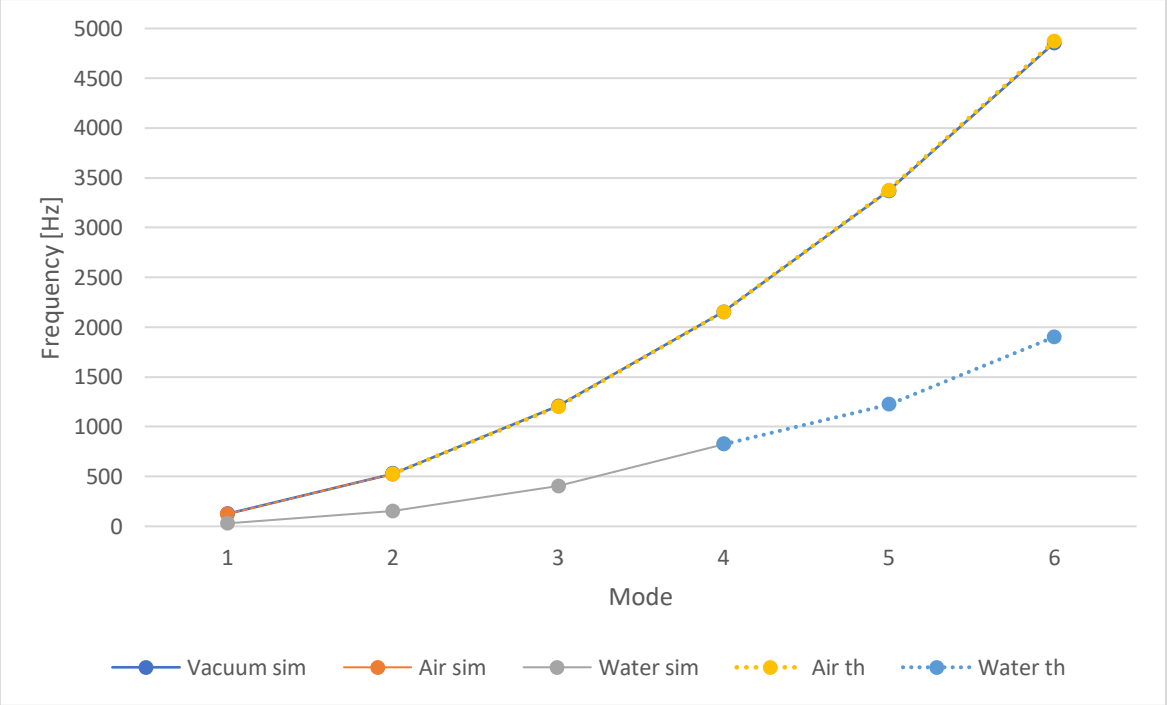

Figure 10. Numerical and theoretical values of the natural frequencies of the axisymmetric modes from s1 to s6.

From the frequency plot in Figure 10, it becomes clear that frequencies reduce when the fluid is water. For the purpose of comparing vacuum, air and water frequency results, theoretical values have been added for the modes that couldn't be found in air and in water, shown in dashed lines. Air frequency evolution comes to be practically the same as in vacuum, which makes sense considering the low density of the fluid. Differently, the water curve increases much smoothly in a far lower range of frequencies, as expected from mass added effects. Despite the percent deviations, water numerical results could be considered to fit with the theoretical ones when compared with the air curve, but a higher agreement between the theory and the simulation is achieved in the latter case.

In order to evaluate those differences, the frequency reduction ratio FRR has been computed according to equation (17) for each mode, considering theoretical values when numerical results are empty.

$$FRR = 100\frac{f_1 - f_2}{f_1} \tag{17}$$

FRR values are indicated in Table 7 for the air-water comparisons. From the plotted values in Figure 11, the ratio decreases the higher the mode although an increase is observed from mode s4 to s5. The average FRR of all the modes is 66,7%.

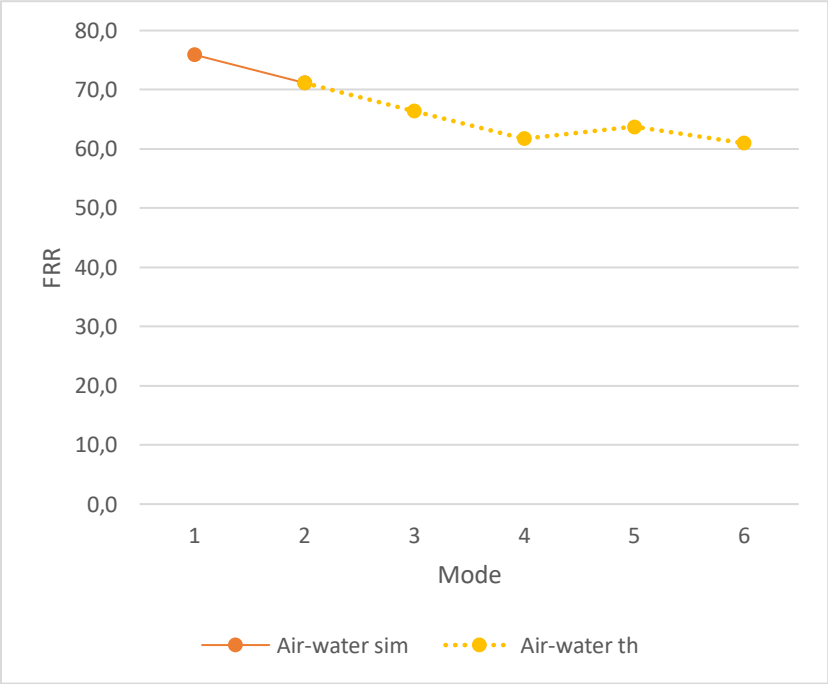

Figure 11. Frequency reduction ratios (FRR) of water compared to air for the axisymmetric modes from s1 to s6, based on numerical and theoretical results

	FRR						$\overline{FRR}$
	Numerical		Theoretical				
Air-water	75,9	71,2	66,4	61,8	63,7	61,0	**66,7**

Table 7. Frequency reduction ratios (FRR) between air and water, based on numerical and theoretical results

Table 8, Table 9 and Table 10 show the radial ratio between nodal circles and the plate radius in vacuum, air and water, respectively. Results are shown for the axisymmetric modes that were numerically found and percent deviations relative to Leissa's theoretical values, exposed in Table 2 of section 4.2, are included. The differences between nodal radii reflect the changes in the mode shape movement, which mostly differs in the water case. Deviations are calculated according to the vacuum theoretical values, so in Table 8 they evaluate the differences between the theory and the simulated results, stating a maximum value of -2,1% in the first nodal circle of the fifth axisymmetric mode. Considered small from s1 to s4 in vacuum, deviations in Table 9 and Table 10 (air and water) rather express the plate's mode shape variations when surrounded by the fluids. In all the cases, higher deviations are observed in the first nodal circle, which refers to the most external one, and all the numerical ratios are below Leissa's ones.

From these results, mode shapes in water appear to change in addition to the frequency reduction in all the modes. Deduced from Table 9 and Table 10, the diameter of the nodal circles reduces when fluid effects are taken into account. In that particular case, the highest reduction is noted in the first nodal circle of the first axisymmetric mode in water, with a value of -10,9%.

Vacuum		r/a					
s1	sim	0,680					
	dev [%]	-0,05					
s2	sim	0,840	0,390				
	dev [%]	-0,3	-0,2				
s3	sim	0,894	0,590	0,258			
	dev [%]	-0,1	-0,2	0,4			
s4	sim	0,918	0,692	0,438	0,192		
	dev [%]	-0,004	-0,05	-0,6	1,2		
s5	sim	0,936	0,752	0,552	0,350	0,156	
	dev [%]	-2,1	-0,1	0,8	-0,3	1,0	
s6	sim	0,945	0,795	0,625	0,460	0,291	0,131
	dev [%]	-1,4	0,1	0,2	1,0	-0,5	-0,1

Table 8. Radii of numerical nodal circles of the plate in vacuum and percent deviations relative to the theoretical values presented in Table 2

Air		r/a	
s1	sim	0,675	
	dev [%]	-0,7	
s2	sim	0,838	0,391
	dev [%]	-0,6	0,05

Table 9. Radii of numerical nodal circles of the plate in air and percent deviations relative to the theoretical in vacuum values presented in Table 2

Water		r/a			
s1	sim	0,606			
	dev [%]	-10,9			
s2	sim	0,780	0,365		
	dev [%]	-7,4	-6,6		
s3	sim	0,848	0,561	0,253	
	dev [%]	-5,3	-5,0	-1,6	
s4	sim	0,880	0,664	0,429	0,191
	dev [%]	-4,1	-4,0	-2,7	0,6

Table 10. Radii of numerical nodal circles of the plate in water and percent deviations relative to the theoretical in vacuum values presented in Table 2

7. Wall distance reduction effects

In this section, the effect of wall proximity is studied when the plate is submerged in water. In particular, the normal distance between the plate and the low wall of the fluid cavity was reduced in order to investigate how the wall disturbed the plate's modes. Starting from the geometry change in SpaceClaim, the wall distance was progressively reduced to 1/2, 1/4, 1/8, 1/16, 1/32 and 1/64 without changing the fluid dimensions in the upper part of the plate (Figure 12). Accordingly, the fluid volume decreased, which made possible to get a slightly better mesh of the acoustic body near the plate. Then, modal acoustic analyses were completed for each distance, following the same steps as in Section 6.

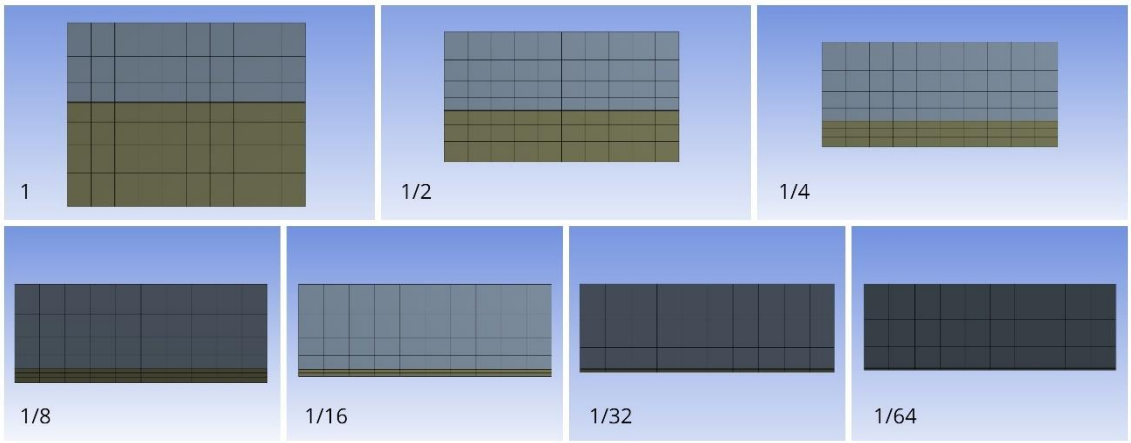

Figure 12. Frontal view of the model for all the wall distances

Facing the same difficulties as before to find the highest modes, only the first 4 axisymmetric modes were reached. In Table 11, frequency results are presented for each wall distance ratio (WDR) and are plotted in Figure 13 and Figure 14. From both figures, it is clearly deduced that frequencies decrease as the plate gets closer to the wall. This agrees with Askari et (2013)[6], who investigated the effects of liquid height and submerged depth on the natural frequencies of a free circular plate. They experimentally observed that the frequencies initially decreased with the immersing depth and became constant when the plate reached the middle of the container. Then, when the plate approached the container rigid bottom, natural frequencies started to decrease again. From the present numerical results, in addition, it is seen that the frequency differences in every mode are also higher in magnitude when the wall distance ratios get smaller, as appears in Figure 14.

	WDR	s1	s2	s3	s4
f_1 [Hz]	1,0000	29,8	151,7	403,6	822,8
$f_{1/2}$ [Hz]	0,5000	29,4	149,2	394,0	794,6
$f_{1/4}$ [Hz]	0,2500	28,9	147,7	389,3	781,5
$f_{1/8}$ [Hz]	0,1250	27,5	144,4	385,1	774,9
$f_{1/16}$ [Hz]	0,0625	24,6	134,4	369,8	758,0
$f_{1/32}$ [Hz]	0,0313	20,6	117,1	333,7	707,1
$f_{1/64}$ [Hz]	0,0156	16,5	95,1	276,9	599,5

Table 11. Numerical results of the natural frequencies of the axisymmetric modes from s1 to s4 in water for different wall distance ratios (WDR)

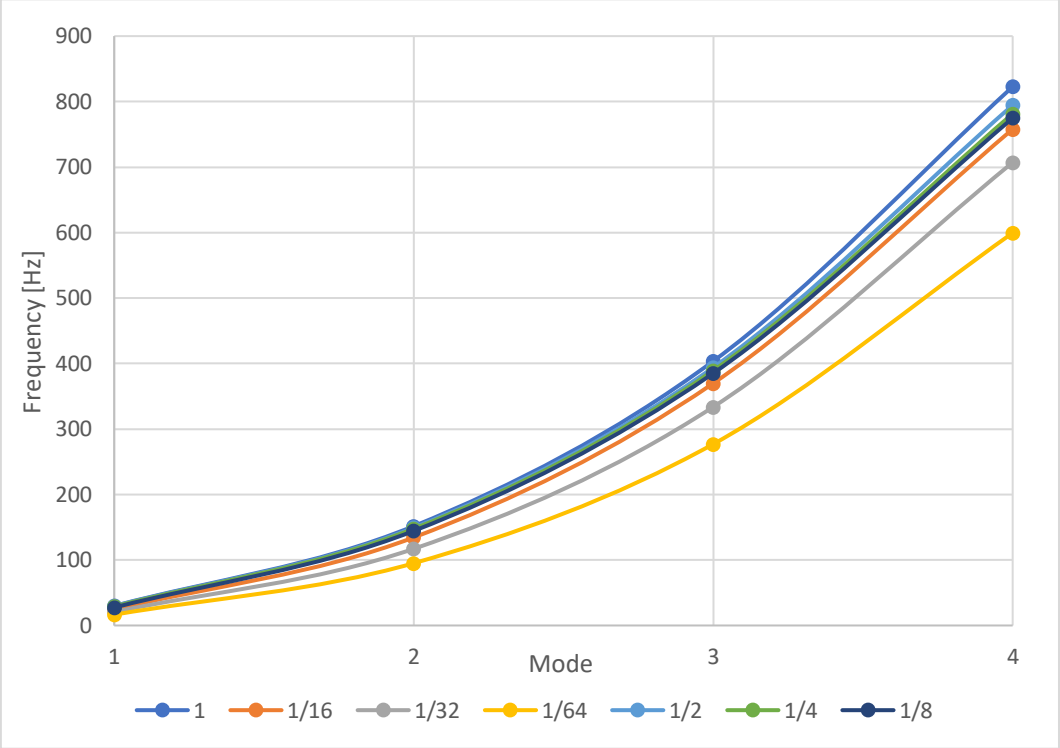

Figure 13. Natural frequency results of the axisymmetric modes in water from s1 to s4 for wall distance ratios of 1, 1/2, 1/4, 1/16, 1/32 and 1/64

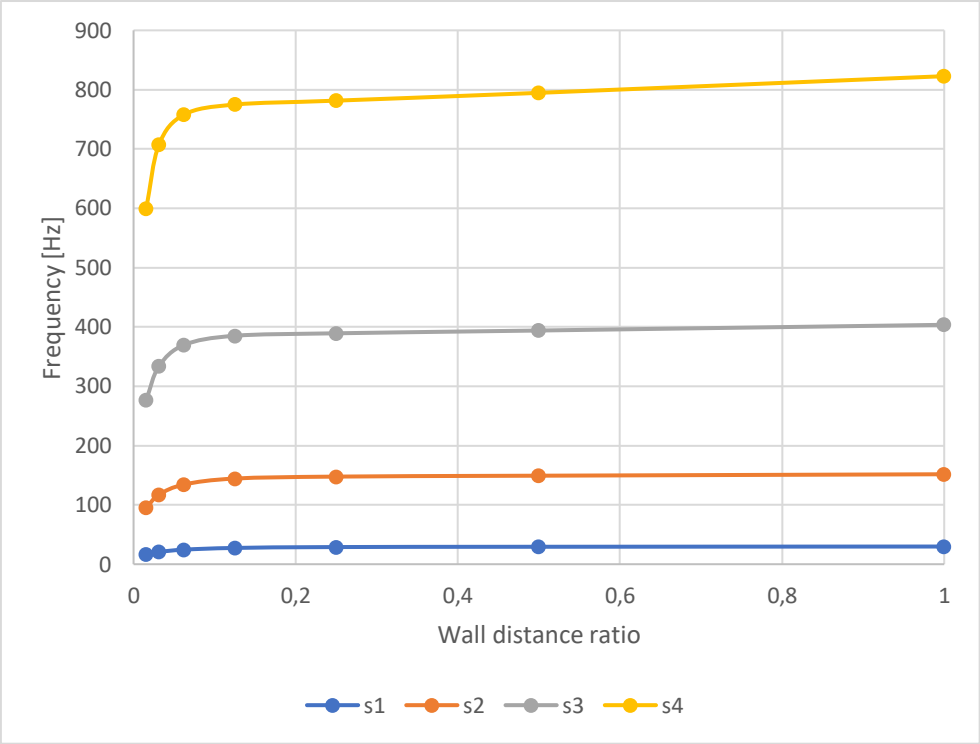

Figure 14. Natural frequency results of the axisymmetric modes in water as a function of the wall distance ratio for s1, s2, s3 and s4

In order to evaluate those frequency reductions, the ratio between every frequency and the highest one in every mode, which concerns to the initial wall distance, was calculated for every separate mode. The resulting values are presented in Table 12 and drawn in Figure 15.

Starting from mode s1, the frequency ratio curve decreases the higher the distance. The same pattern would be expected in higher modes with higher values, but little variations are observed. So as to clearly observe those differences, the logarithmic function of the frequency ratio (FR) has been plotted in Figure 16. The concerning values are presented in Table 13.

	WDR	s1	s2	s3	s4
FR_1	1,0000	1	1	1	1
$FR_{1/2}$	0,5000	0,987	0,984	0,976	0,966
$FR_{1/4}$	0,2500	0,971	0,974	0,965	0,950
$FR_{1/8}$	0,1250	0,921	0,952	0,954	0,942
$FR_{1/16}$	0,0625	0,824	0,886	0,916	0,921
$FR_{1/32}$	0,0313	0,692	0,772	0,827	0,859
$FR_{1/64}$	0,0156	0,552	0,627	0,686	0,729

Table 12. Frequency ratio (FR) from s1 to s4 for every wall distance ratio

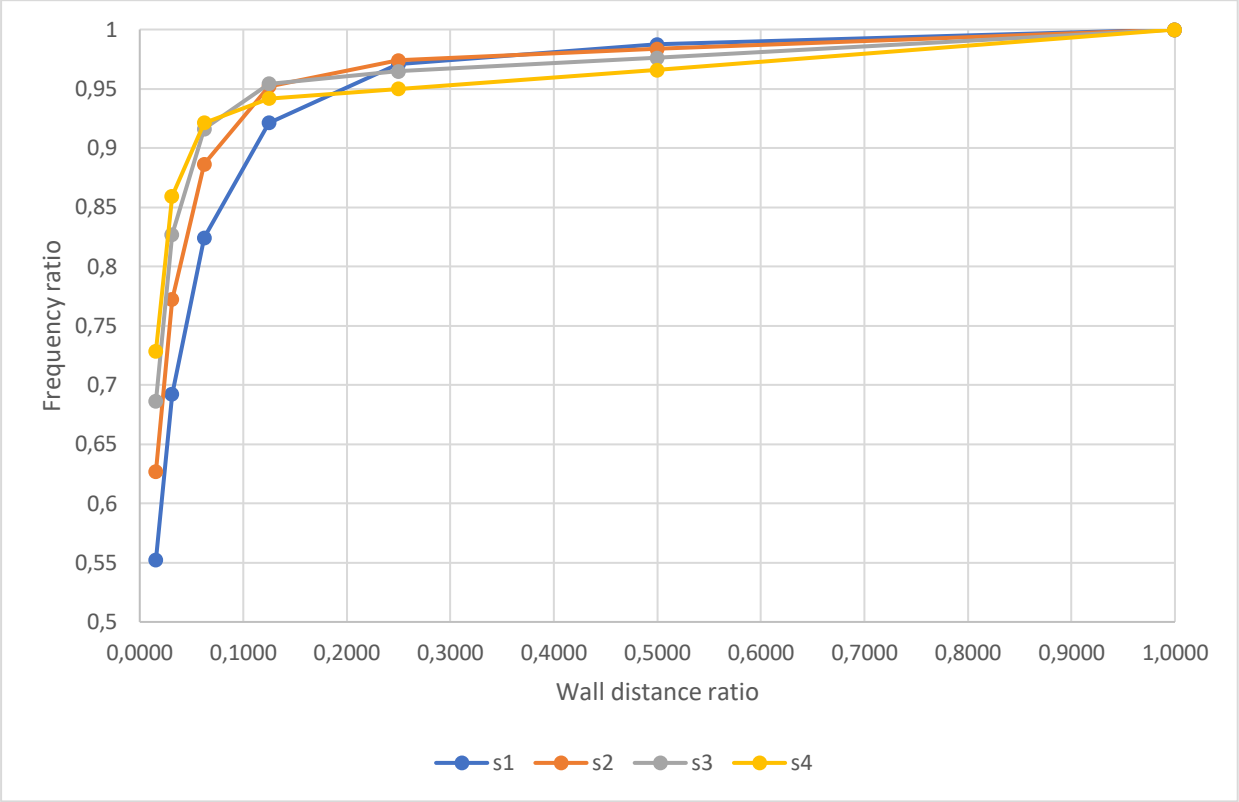

Figure 15. Frequency ratio as a function of the wall distance ratio for s1, s2, s3 and s4

As shown in Figure 16, similar logarithmic patterns are observed in small distances, but with bigger FR the higher the mode as already noticed before. However, in higher distances, the logarithmic curve changes, especially in increasing modes. Looking at mode s4, it is clearly observed that the function rises instead of turning down in the 0,5 and 1 distance ratio points. The same occurs in mode s3 but more slightly, as the higher the mode the more noticeable are these variations.

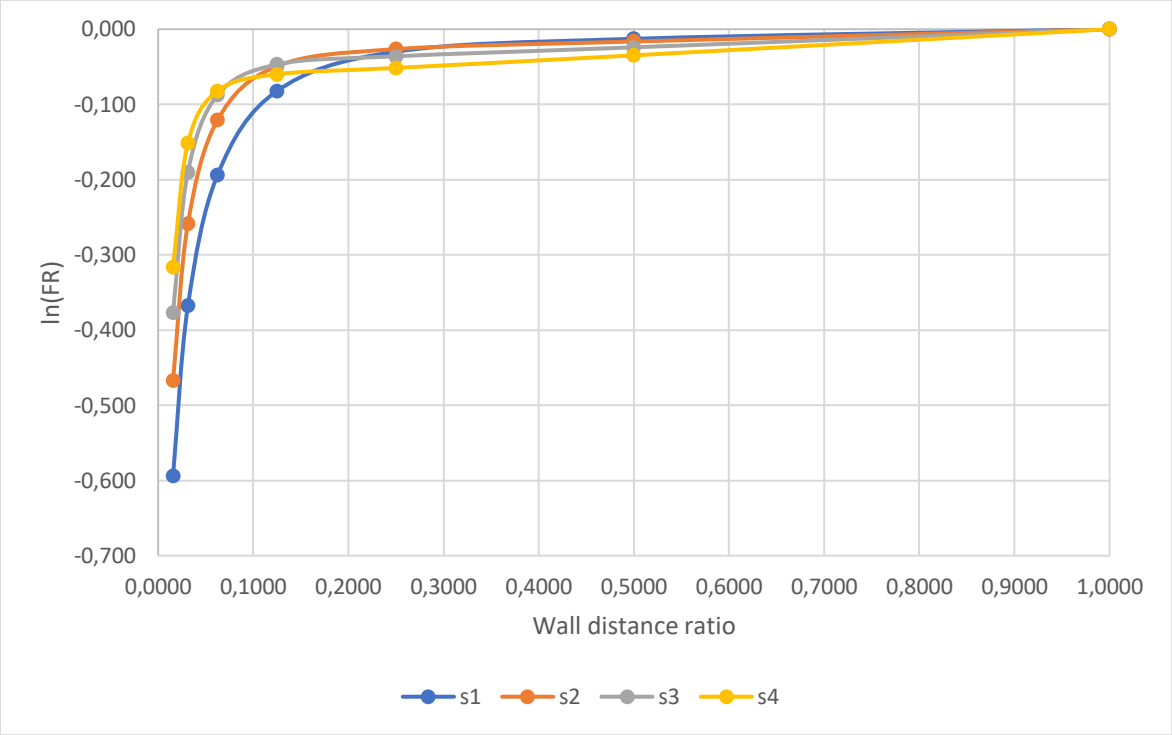

Figure 16. Logarithm of the frequency ratio (FR) as a function of the wall distance ratio for s1, s2, s3 and s4

	WDR	s1	s2	s3	s4
$\ln(FR_1)$	1,0000	0,000	0,000	0,000	0,000
$\ln(FR_{1/2})$	0,5000	-0,013	-0,016	-0,024	-0,035
$\ln(FR_{1/4})$	0,2500	-0,030	-0,026	-0,036	-0,051
$\ln(FR_{1/8})$	0,1250	-0,082	-0,049	-0,047	-0,060
$\ln(FR_{1/16})$	0,0625	-0,193	-0,121	-0,088	-0,082
$\ln(FR_{1/32})$	0,0313	-0,368	-0,259	-0,190	-0,151
$\ln(FR_{1/64})$	0,0156	-0,594	-0,467	-0,377	-0,317

Table 13. Values of the frequency ratio (FR) logarithm for each wall distance ratio from s1 to s4

8. Two-way coupled analysis

This section introduces a more complex type of simulations that combine Mechanical APDL and CFX solvers to solve transient FSI problems. In these analyses, both solvers work at the same time, but are coordinated through a System Coupling component that transfers solution data to each other. Thus, the solution process takes into account not only the actions of the fluid and the structure in the whole system, but also the interaction that occurs between them. To do so, the motions of the structure and the fluid must be modelled separately and then they are connected through the coupling system. In this case, the plate's deformation was calculated using a Transient Structural analysis system from the Mechanical APDL applications, while the air and the water motions were computed with Fluid Flow analysis systems from CFX.

The two-way coupling involves two data transfers. On one hand, force data from the fluid's motion is received by the structural analysis system as it solves the plate's behaviour over time. On the other, displacement data from the motion of the plate is received by the fluid analysis system as the fluid behaviour is being solved. Then, both solutions are the result from the coupled combination as a one. Figure 17 shows the two-way coupling system that was built with the appropriate connections. The setup cells were connected and a common geometry was defined using the model that had already been designed. In the Transient Structural analysis, the Engineering Data cell was also reused from previous work where material properties had already been introduced.

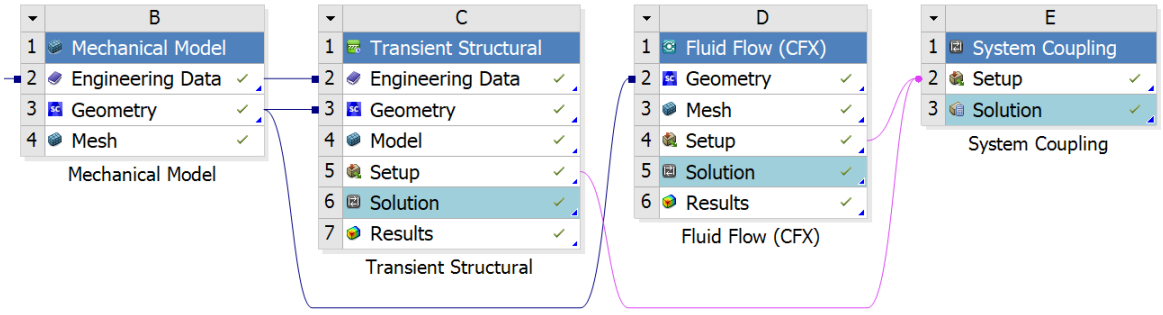

Figure 17. Two-way coupling system project schematic

On another hand, in any time dependent analysis, the duration of the simulation and the time step are variables that must be accordingly defined. The time step refers to the size of the time increments that are being solved within the transient analysis, so the sum of the time step calculations conforms the complete solution. In this problem, it was important that the time step was fine enough to see the plate's oscillations to a reasonable degree. However, coupling solutions weren't reached for a good equilibrium between time variables and the frequency force, as it will be discussed later. As a consequence, a general time duration of 10 seconds and a time step of 0,1 seconds were set.

8.1. Defining the Structural Analysis System

Once the geometry was set, the mesh of the Transient Structural analysis system was generated in the Mechanical application. As this part of the coupled system would only focus on the plate's motion, the geometry of the fluid had to be excluded and fixed as "Suppressed Bodies" in the structural analysis. Then, the mesh of the plate was completed as in previous analyses.

The next step was to define the loads and the analysis settings. Only 1 step and 1 substep were set, with a "Step End Time" of 10 seconds as the total time of simulation. On another hand, the Fluid Solid Interface was defined selecting all the faces of the plate. Then, the sinusoidal force was introduced as a function of time with the following expression, in N:

$$F = \sin(t \cdot 360f) \tag{18}$$

where t is time and f is the frequency in Hz at which the plate is being excited. As Ansys works in degrees, the angular velocity needed to be defined as $360f$.

However, the current system had too many degrees of freedom to be solved, so it was necessary to apply an external condition. In order to unable the execution of the simulation, the inner faces of the plate (the hole faces) were decided to be fixed using the "Cylindrical Support" condition. As a consequence, the characteristics of the system were forced to change and the plate would no longer be a completely free plate, but a centre-fixed plate. Therefore, the natural frequencies of the plate were calculated again with modal acoustic analyses but applying the same fixing condition. Table 14 shows the new natural frequencies of the fixed plate in vacuum, in air and in water.

Mode	s1	s2	s3	s4	s5	s6
f_{vacuum} [Hz]	52,6	295,0	855,2	1691,3	2807,4	4202,2
f_{air} [Hz]	52,4	297,1	867,9			
f_{water} [Hz]	9,6	68,4	245,0	574,6		

Table 14. Numerical results of the axisymmetric natural frequencies in vacuum, air and water for the circular plate fixed at its centre

For these frequencies, a new total time of simulation with an appropriate time step should be adjusted in order to visualize the plate's oscillations. Figure 18 and Figure 19 show the details of the force relative to the first axisymmetric mode in water (9,567 Hz) and the sinus plot as a function of time. A reasonable simulation time would be of 0,5 seconds, which would allow to visualize 5 oscillations. Then, timestep should be around 0,005 seconds.

Details of "Force"

Scope	
Scoping Method	Geometry Selection
Geometry	4 Faces
Definition	
Type	Force
Define By	Components
Applied By	Surface Effect
Coordinate System	Global Coordinate System
X Component	0, N (step applied)
Y Component	= sin(time*3444,12)
Z Component	0, N (step applied)
Suppressed	No
Function	
Unit System	Metric (m, kg, N, s, V, A) Degre...
Angular Measure	Degrees
Graph Controls	
Number Of Segments	200,

Figure 18. Details of the force applied to the plate in the Transient Structural analysis system

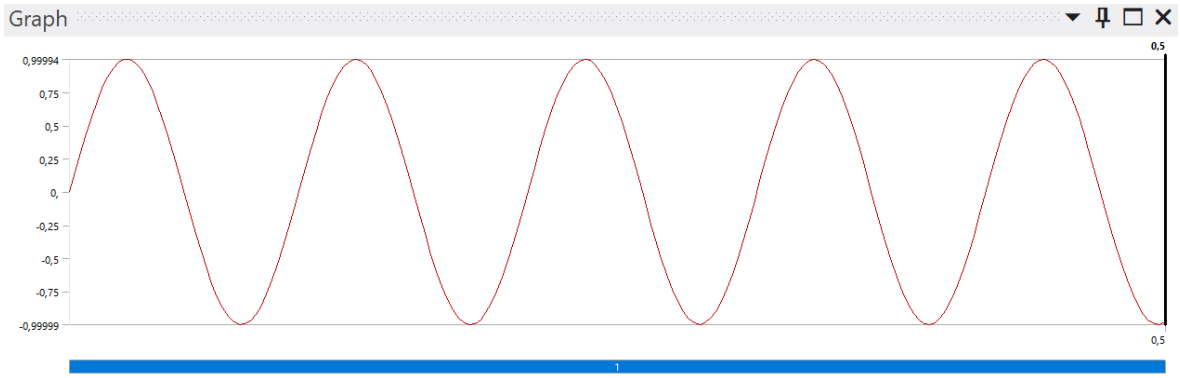

Figure 19. Plot of the sinusoidal force applied in the Transient Structural analysis system as a function of time

8.2. Defining the Fluid Flow (CFX) Analysis System

Having the geometry already defined, the first step to do in the Fluid Flow analysis system was to generate the mesh. The mechanical application was opened as in the structural system and the mesh was completed as in previous analyses. This time, though, the plate's body was suppressed and the mesh was done only for the fluid remaining bodies. On another hand, Named Selections were created in order to ease the setting up of the fluid analysis that would go next. The new named selections were: the wall deforming top (Figure 20), the wall deforming lateral (Figure 21), the wall deforming bottom (Figure 22), the wall top (Figure 23) and the wall closed (Figure 24).

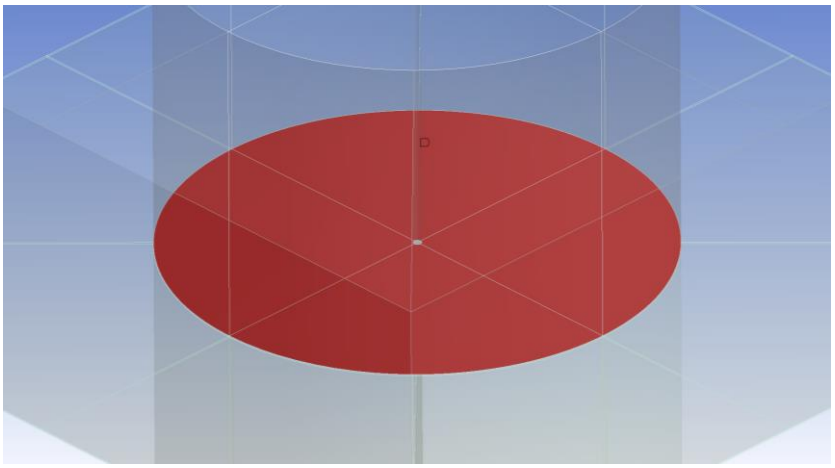

Figure 20. Wall deforming top

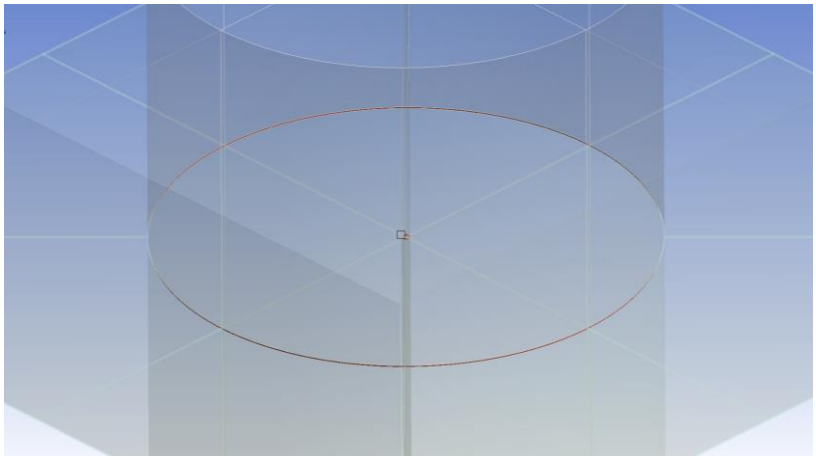

Figure 21. Wall deforming lateral

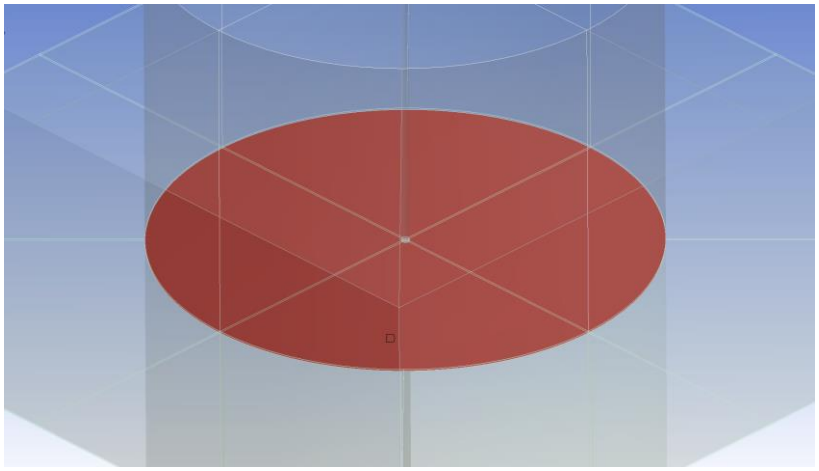

Figure 22. Wall deforming bottom

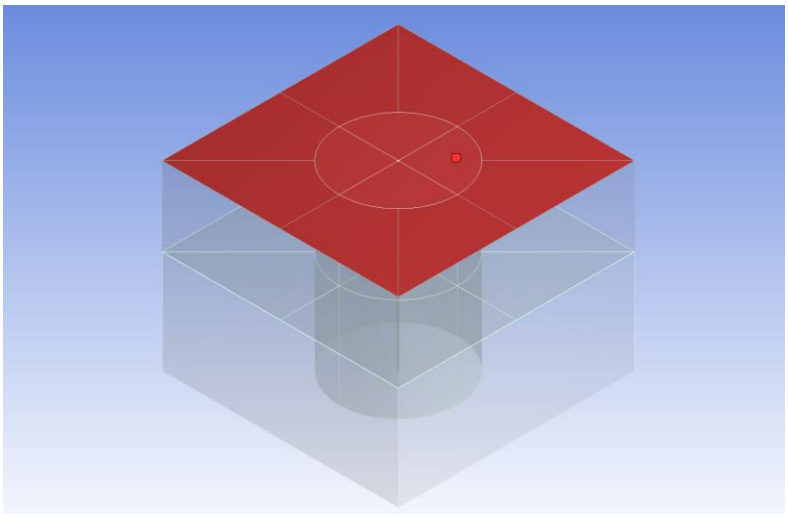

Figure 23. Wall top

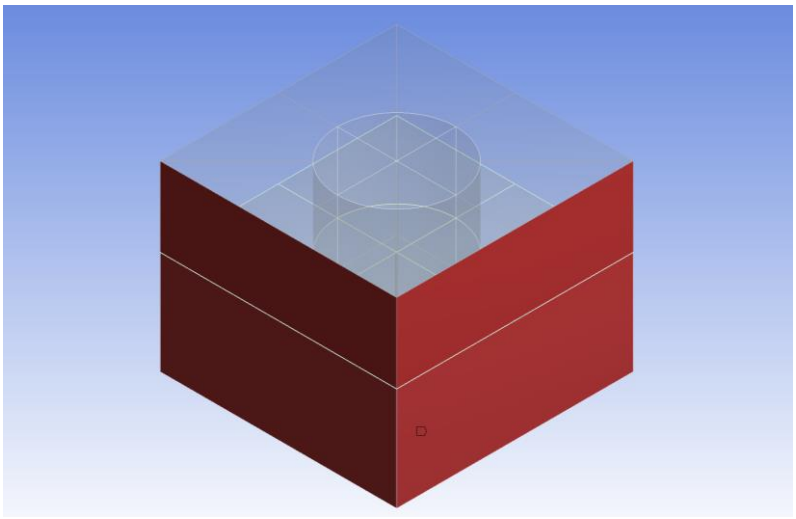

Figure 24. Wall closed

Then, CFX-Pre was launched to set up the analysis and to define the fluid interface. First of all, the transient analysis was specified with the total time and the timestep that had already been decided in the structural analysis. So as to enable the Ansys Mechanical solver to communicate mesh displacements to CFX-Solver, mesh motion was activated by creating the domain. The location was assigned to all the fluid parts and the fluid material was selected (air or water). The reference pressure was set to 1 atm. On another hand, mesh deformation was determined in “Regions of Motion Specified”, with displacement relative to previous mesh. Then, the mesh motion model was defined with the “Displacement Diffusion” option: the mesh stiffness was set to increase near small volumes with a ratio of 2 and the reference volume was assigned to the “Mean Control Volume”. In the fluid model settings, no heat transfer nor turbulence (laminar) options were applied.

Once the default domain was defined, the boundaries were created. In this case, two types of boundaries are necessary: the fluid solid external boundary, which results from the fluid-solid interface, and the symmetry boundaries. In the CFX-Solver, the interface between Ansys Mechanical and CFX is considered as an external boundary whose displacement is defined by the coupling system. On this boundary, CFX-Solver sends the forces on the interface to Ansys Mechanical solver, which then sends back the mesh displacement resulting from the CFX forces and the structural loads defined. The interface boundary was defined in the wall deforming location, that is, in the “wall deforming top”, the “wall deforming bottom” and the “wall deforming lateral” named selections that were previously created. It was specified as a “no slip wall” boundary type with mesh motion coming from System Coupling. The same type of wall boundary was assigned to the “wall closed” location, which in a hypothetical experimental case it would be in contact with a rigid tank. Finally, the “wall top” faces were described as an opening boundary with stationary mesh motion and relative pressure of 0 Pa.

Any transient simulation needs initial values for all variables. In this case, all velocity cartesian components were initialised at 0 m/s, as well as the relative pressure at 0 Pa. These settings would ensure that the fluid is initially at rest and that the flow is generated by the plate motion.

Finally, solver settings must be selected according to the type of simulation. Within each time step, a series of stagger iterations are performed to make sure that both the CFX and the Mechanical solvers and the data exchanged between them are consistent. In every stagger iteration, the two solvers run once each, but the user can specify which one runs first in the Solver Settings. In this case, as the simulation is being started by the force applied to the plate, the Mechanical application was set to solve before the CFX. Following Ansys tutorial indications [11], Upwind and Second Order Backward Euler schemes were selected with automatic timestep initialisation and Velocity Pressure Coupling was included as advanced options. Relative to convergence controls, a minimum of 1 and a maximum of 5 coefficient loops were set with a residual target of 1e-4 RMS. Then, pressure and velocity were introduced as output variables, saving the transient results every timestep. Lastly, the CFX solver was chosen to run in double precision.

8.3. Defining the coupling in the System Coupling application

First of all, the System Coupling must be set up with the analysis settings decided for the simulation. In accordance, the end time and the timestep introduced were 0,5 seconds and 0,005 seconds, respectively, the same as defined in the structural and fluid systems.

As previously explained, the two-way coupled analysis implies that solutions from the structural and the fluid systems are constantly shared by means of the System Coupling component. Consequently, in the System Coupling Settings, Data Transfers must be clearly defined because they coordinate the whole solution process. Thus, two data transfers were created between the Fluid Solid Interface region (from the structural system) and the wall deforming region (from the Fluid system). In the first one, the surface of the structural system around the plate would transfer displacements to the surface around the plate of the fluid system, so the Transient Structural and the Fluid Flow (CFX) systems would be the source and the target participants, respectively. In the other, the surface of the fluid system around the plate would transfer force to the surface around the plate of the structural system, so participants were assigned contrarily.

8.4. Solving the two-way coupled analysis

Once the setup of both the Transient Structural and the Fluid Flow (CFX) analysis systems were updated, the simulation was launched through the System Coupling Solution cell. Disappointingly, no solutions were achieved for the desired frequencies as the solver was unable to converge with the appropriate settings. Figure 25 shows common errors that the solver encountered in several trials. Displacements and the frequencies applied were found too high for the centre-fixed circular plate, so either the system or the forces introduced would have to be changed.

Error!	Update failed for the Solution component in System Coupling. The coupled update for system Fluid Flow (CFX) threw an exception. The solver failed with a non-zero exit code of : 2
Error!	(DP 0) A solver failure occurred during the run in the Fluid Flow (CFX) system
Error!	(DP 0) An internal solution magnitude limit was exceeded. Please check your Environment for inappropriate load values or insufficient supports. Please see the Troubleshooting section of the Help System for more information.
Error!	(DP 0) An internal solution magnitude limit was exceeded. Please check your Environment for inappropriate load values or insufficient supports. Please see the Troubleshooting section of the Help System for more information.
Error!	(DP 0) An internal solution magnitude limit was exceeded. Please check your Environment for inappropriate load values or insufficient supports. Please see the Troubleshooting section of the Help System for more information.
Warning!	(DP 0) The unconverged solution (identified as Substep 999999) is output for analysis debug purposes. Results at this time should not be used for any other purpose.
Error!	(DP 0) An internal solution magnitude limit was exceeded. (Node Number 1316, Body Plate, DOF UY) Please check your Environment for inappropriate load values or insufficient supports. You may select the offending object and/or geometry via RMB on this warning in the Messages window. Please see the Troubleshooting section of the Help System for more information.
Error!	(DP 0) Participant Solution 1 encountered a fatal error. Message: The value of UY at node 1316 is 8.362633577E+39. It is greater than the current limit of 1000000 (which can be reset on the NCNV command). This generally indicates rigid body motion as a result of an unconstrained model. Please do not save the project if you would like to recover to the last saved state.

Figure 25. Error messages emerged from failed solutions

However, changing the time parameters, one complete simulation of the first axisymmetric mode in water was achieved. Although the time duration and the timestep selected weren't the desired at all, solution results could be observed. Still, with 0,5 seconds of total duration and a timestep of 0,05 seconds, no consistent conclusions could be taken from the results, as too many calculations were missing. Figure 26 shows the deformation plot of the plate, which clearly appears with insufficient data points for a sinusoidal movement.

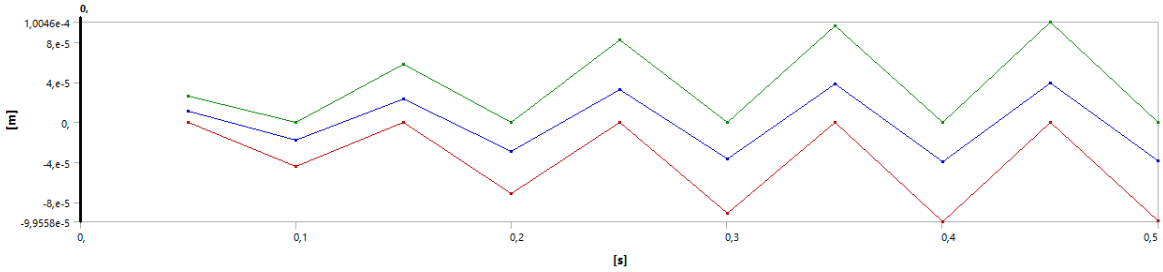

Figure 26. Deformation of the plate as a function of time of the 0,5 s total simulation with timestep of 0,05 seconds

To face all these problems, a new strategy was taken. As one of the principal objectives of the project was the testing of the two-way coupled simulations, the frequencies were decided to be changed. Considering the computational effort that this type of analyses need and the available tools that I had to go forward, I found more interesting for the future to achieve one satisfactory solution that could help to understand how the application works. Thus, the frequencies introduced in the forces applied on the plate were reduced setting aside the excitement of the plate at its axisymmetric modes.

8.5. Two-way coupled analysis results

For a general two-way coupled analysis, frequencies were set in a standard range from 0,1 Hz to 5 Hz. As an example, exciting the plate at 0,167 Hz would be relative to applying the following sinusoidal force:

$$F = \sin(60t) \tag{19}$$

Then, a total simulation time of 10 seconds and a timestep of 0,1 seconds would allow to visualize two oscillations of the plate in water, as shown in Figure 27.

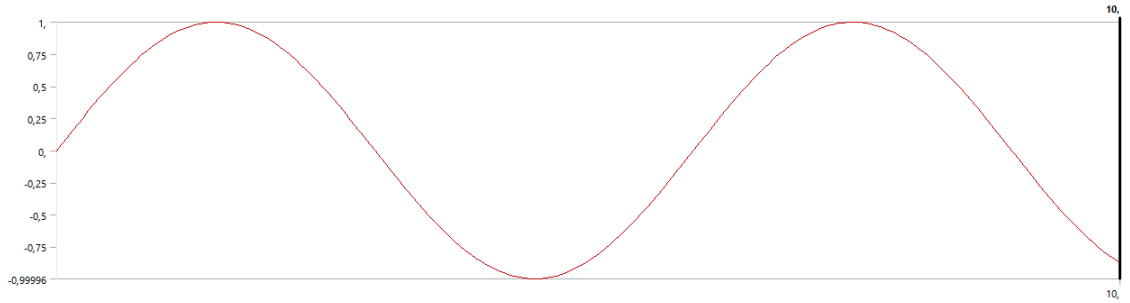

Figure 27. Plot of the sinusoidal force from (19) as a function of time along the total simulation of 10 seconds

Changing these parameters, the solver was able to complete one total simulation. Solutions from the Mechanical and the Fluid Flow (CFX) systems can be visualized independently, but the whole system motion, including the plate and the fluid bodies, can be also studied through CFX-Post. Dragging the Solution cell from Transient Structural to the Results cell of the Fluid Flow (CFX), displacement results from the plate are added to the post-processing application of CFD, which includes the fluid's results and many different tools to graphically view the solutions in 3D. From the Mechanical application, Figure 28 shows the structural deformation plot of the plate from the coupling solution.

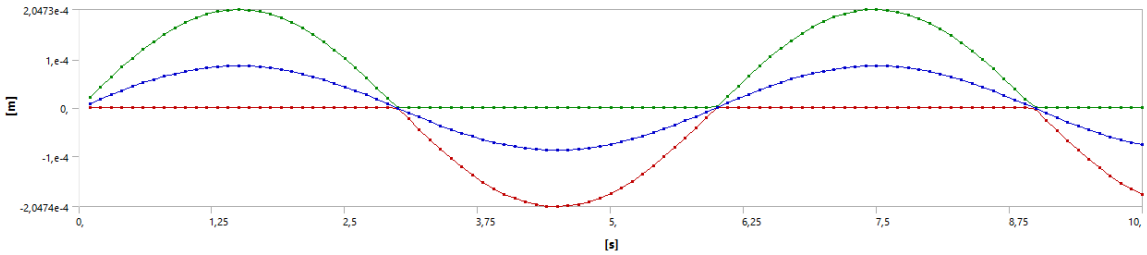

Figure 28. Results of the maximum (green), minimum (red) and average (blue) deformations of the plate in the total simulation of 10 s and timestep 0,1 s

In CFD-Post, captures of the solutions of the total system were done at different timesteps of the simulation. As the total time was 10 seconds and the timestep size was 0,1 seconds, solution results were available at a total of 101 timesteps (from 0 to 100). Using post-processing tools, results were visualized and drawn as convenient. In Figure 29, solutions are shown at timestep 1 (t=0,1s). On the plate's faces, Von Mises Stress were plotted to indicate the elastic deformation state of the structure. The "Default Boundary" concerns to the boundary limit of the plate, whose results come from the Mechanical application. On another hand, a transversal XY plane was created (Plane 1) so as to visualize the fluid's results. Velocity was displayed using a vector plot to indicate the magnitude and the

direction of velocity at every point of the fluid. Then, with a contour plot, pressure levels were drawn in the background of Plane 1.

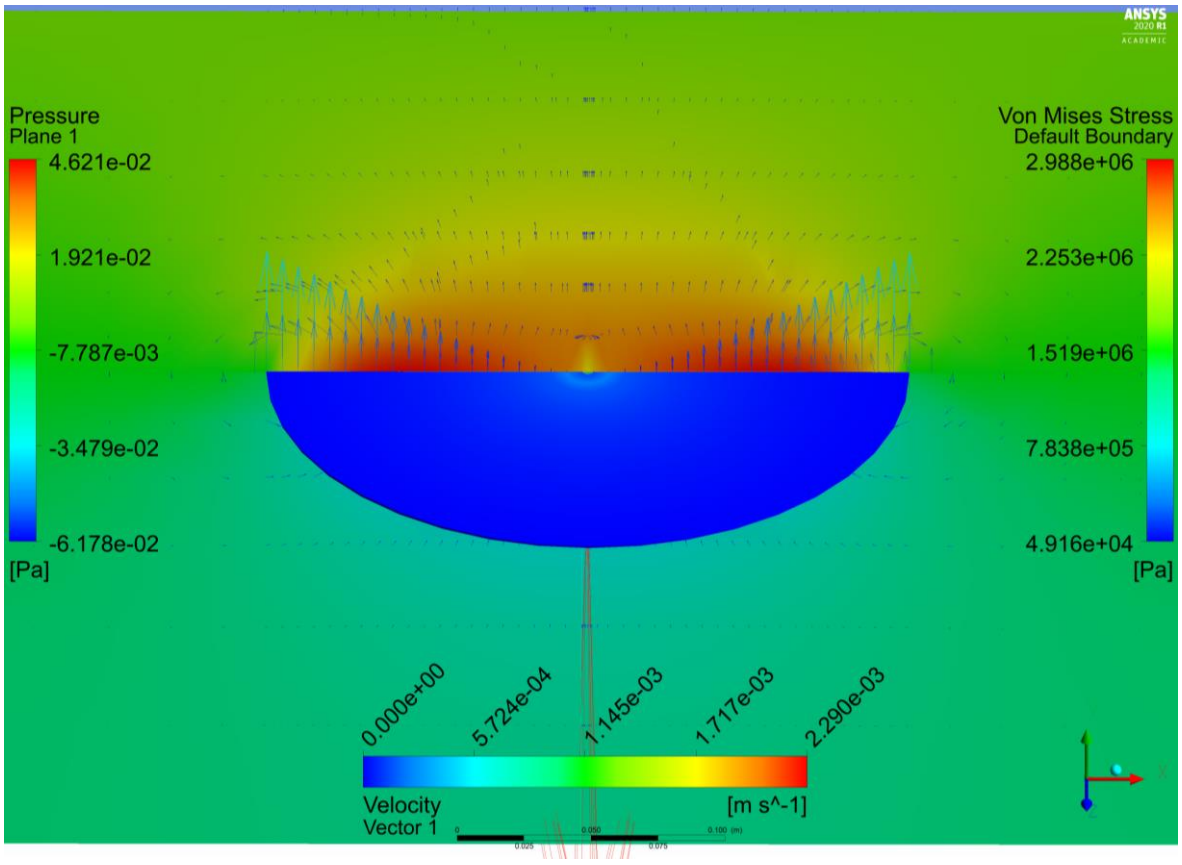

Figure 29. Graphical results of the pressure, velocity and Von Mises Stress at timestep 1 (t=0,1s)

When the simulation starts, pressure values in the fluid area above the plate increase due to the start of motion, as seen from Figure 29 at timestep 1. In the next two timesteps, represented in Figure 30 and Figure 31, pressure levels rapidly decrease and stay widely constant along the whole simulation, with little variations that depend on the sinusoidal state of the plate.

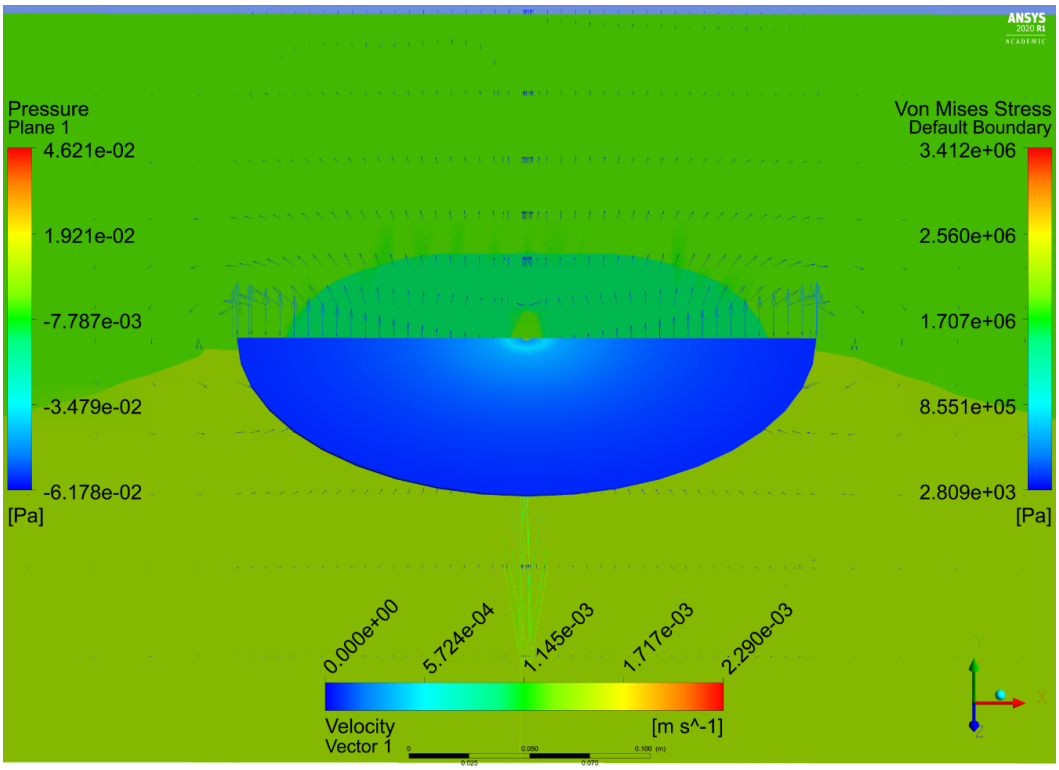

Figure 30. Graphical results of the pressure, velocity and Von Mises Stress at timestep 2 (t=0,2s)

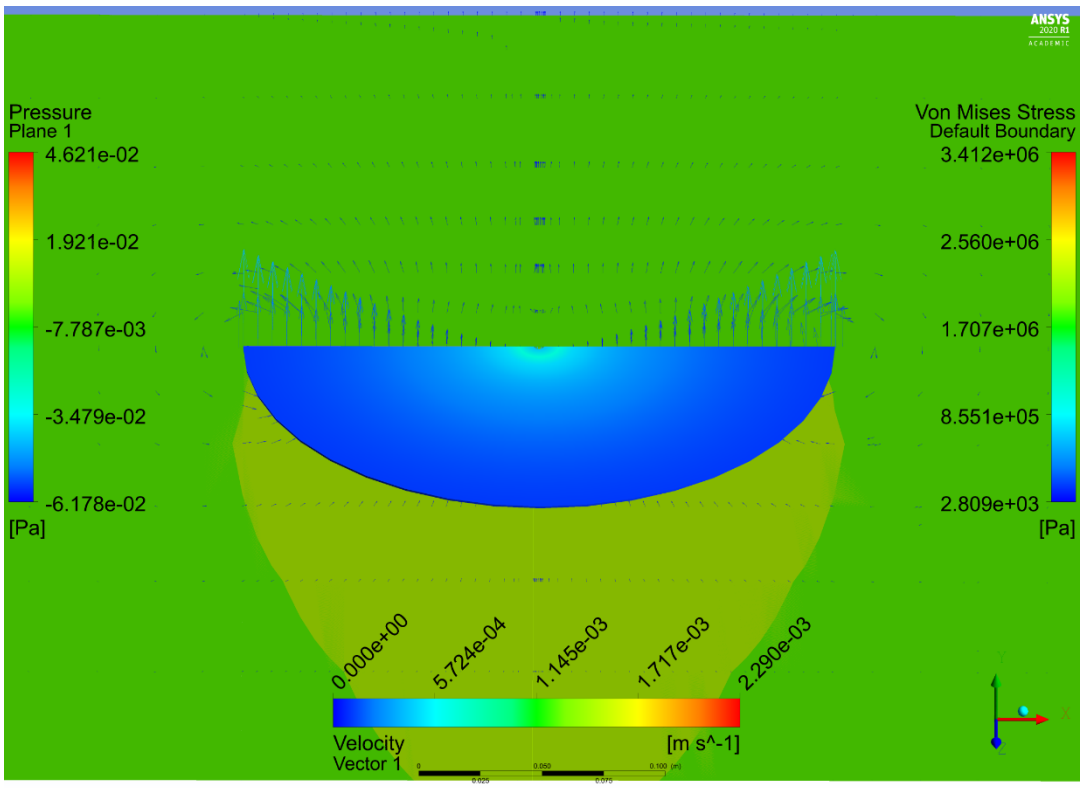

Figure 31. Graphical results of the pressure, velocity and Von Mises Stress at timestep 3 (t=0,3s)

Figure 33 shows the sequence of captures from the beginning of the simulation (t=0s) until the end (t=10s). It starts from timestep 0 and goes until the end with an incremental interval of 5 timesteps (0,5s). On another hand, in Figure 32, captures at every second of the simulation have been included in the plate's deformations plot, so results can be easily related with the deformation and the movement of the plate.

As seen from both figures, the highest Von Mises Stress concentrate in the central part of the plate that surrounds the cylindrical support when deformation values are maximum. Those instants concern to the maximum values of the sinusoidal applied load, and so when the plate is flexed the most because of the inner fixed faces (timesteps 15, 45 and 75). When the force becomes 0, the plate is no longer deformed and consequently Von Mises Stress goes to 0 (timesteps 30, 60 and 90).

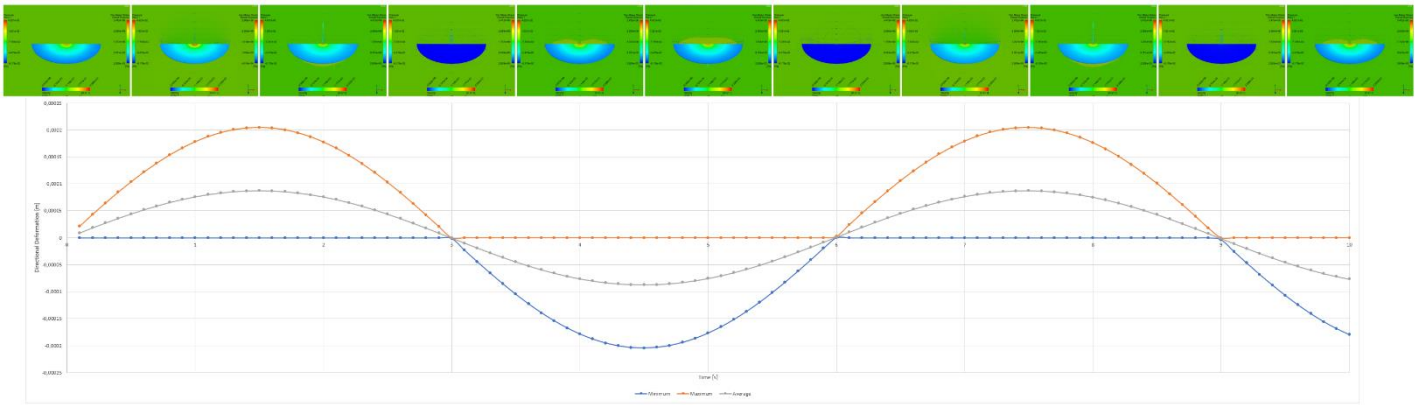

Figure 32. Graphical results' evolution along the total simulation, related to the deformation state of the plate.

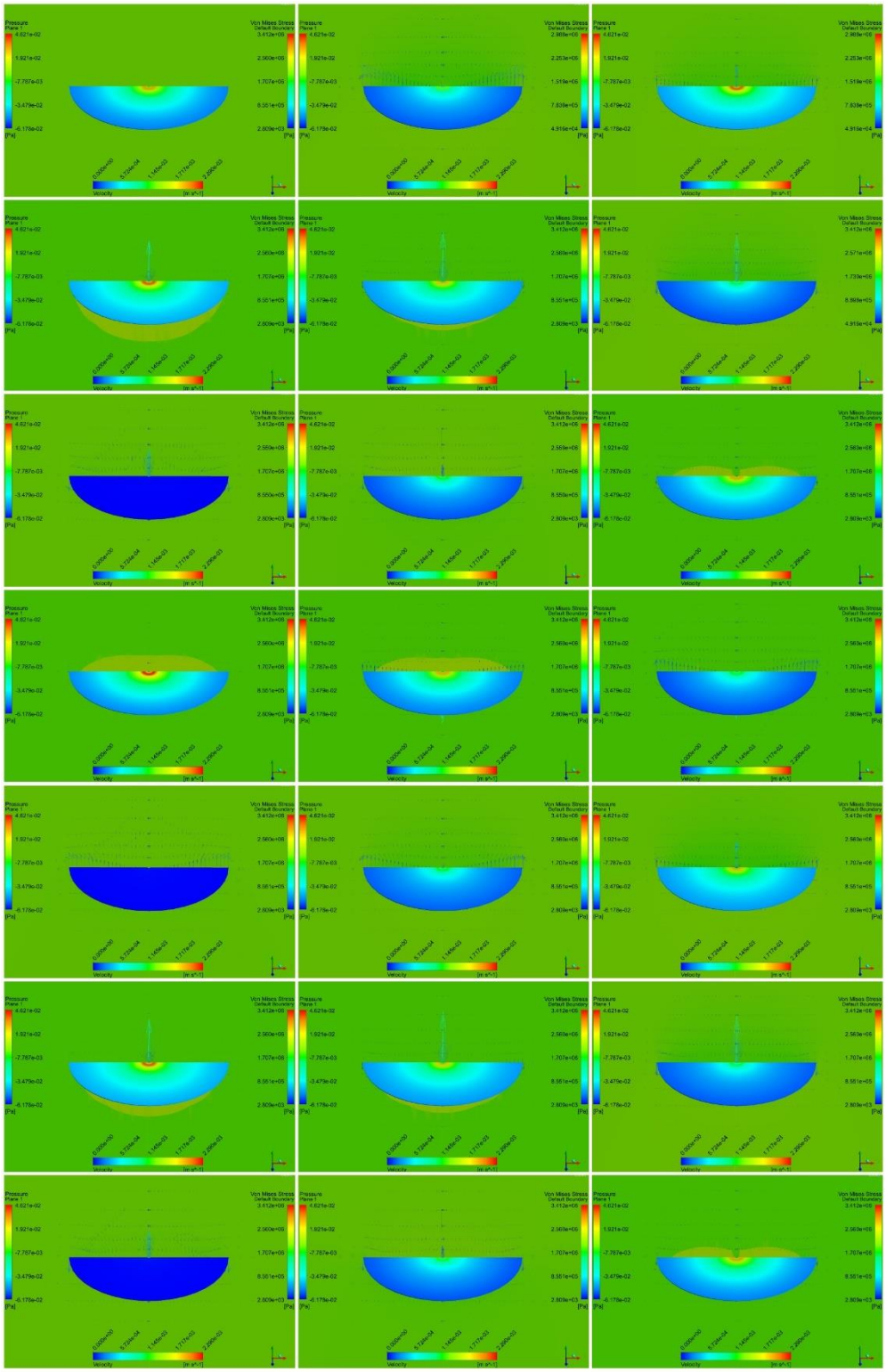

Figure 33. Graphical results evolution along the total simulation from t=0s until t=10s, with a timestep increase interval of 5 timesteps (0,5 s)

Regarding to the fluid's velocity, the maximum values around the plate appear when the sinus slope is maximum in the perimetral areas of the plate, as these are the parts that have higher displacement when scrolling up and down. However, due to the model fixed condition, a fluid flow slips through the small central hole. This central flow compensates the fluid's changing velocity that varies according to the movement of the plate.

When the plate is not deformed, that is, when velocity around the plate is maximum, the central flow compensates the movement of fluid mass in the contrary direction (t=3s, Figure 34). However, as the plate starts to deform, the inverse flow starts to decrease because on the plate there's more space for the fluid to move on. At t=3,5s (Figure 35), the inverse velocity in the centre is small and velocity vectors that go with the plate's deformation direction start to appear. At t=3,6s (Figure 36), these velocity vectors overcome in magnitude the inverse flow, which finally disappears at t=4s (Figure 37). At this moment, the fluid's velocity around the plate has decreased considerably, as the plate is about to arrive to the maximum deformation (at t=4,5s, Figure 38). As long as the general fluid velocity is reduced, the central flow increases balancing the fluid's mass that needs to move. When the maximum deformation is passed by, the plate starts to move in the contrary direction towards its initial position. Accordingly, the fluid's velocity around the plate increases in the same direction. At t=5,7s (Figure 39) the velocity vectors of the now contrary central flow reach their maximum value and then start to decrease. At this moment, the plate's velocity, and so the average fluid's one, are about to get maximum. Finally, at t=6s (Figure 40) the initial position is restored and maximum velocity around the plate is reached again.

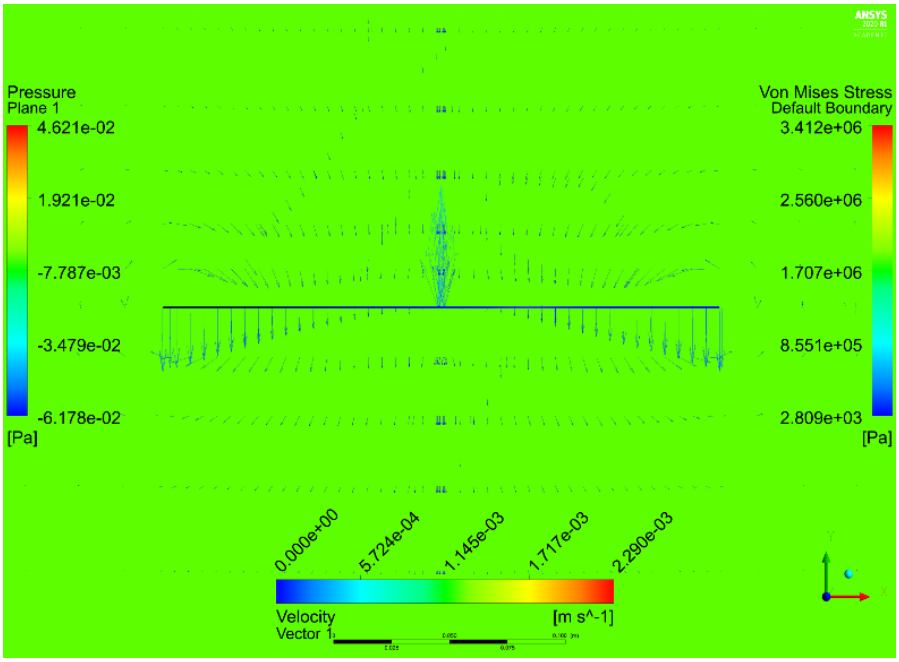

Figure 34. Frontal display of the graphical results at timestep 30 (t=3s)

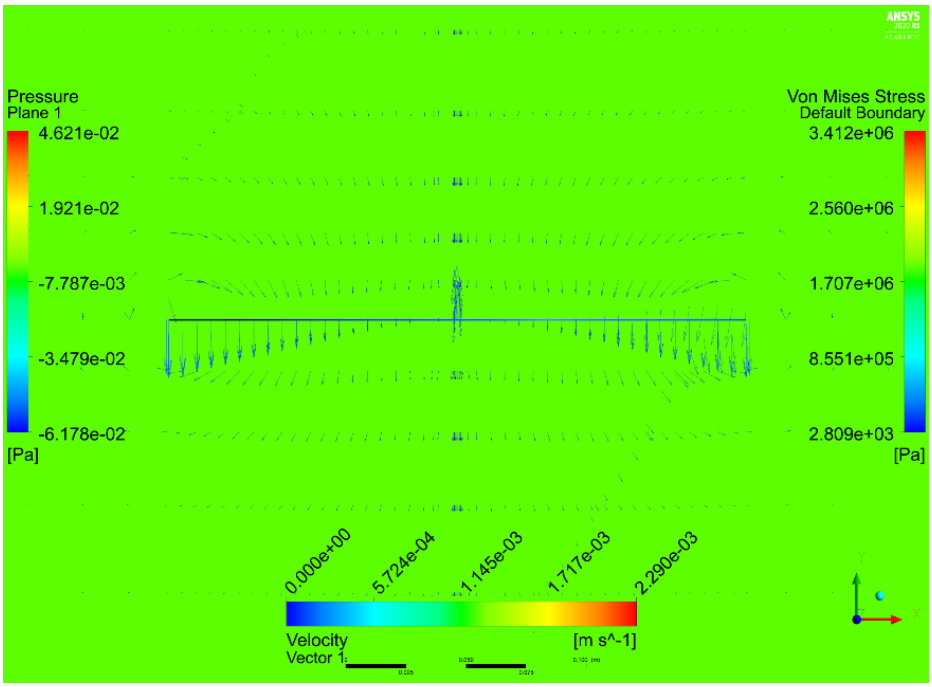

Figure 35. Frontal display of the graphical results at timestep 35 (t=3,5s)

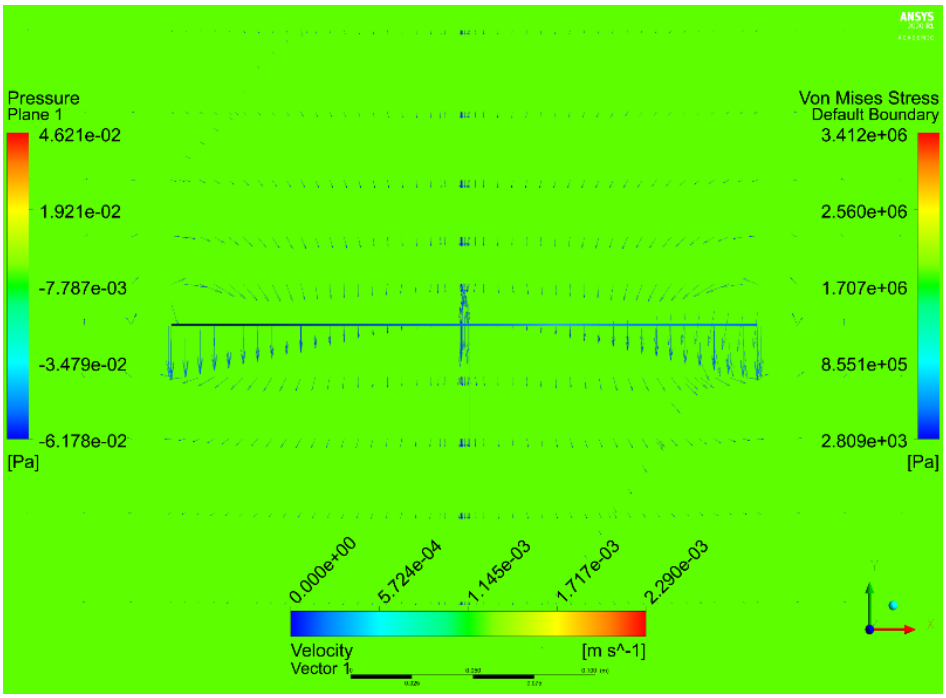

Figure 36. Frontal display of the graphical results at timestep 36 (t=3,6s)

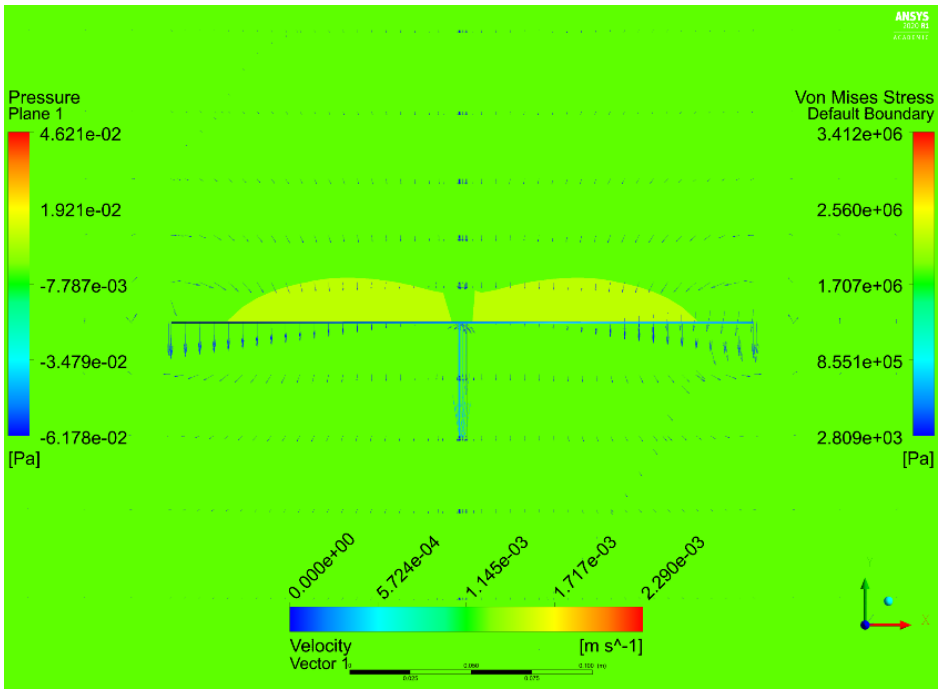

Figure 37. Frontal display of the graphical results at timestep 40 (t=4s)

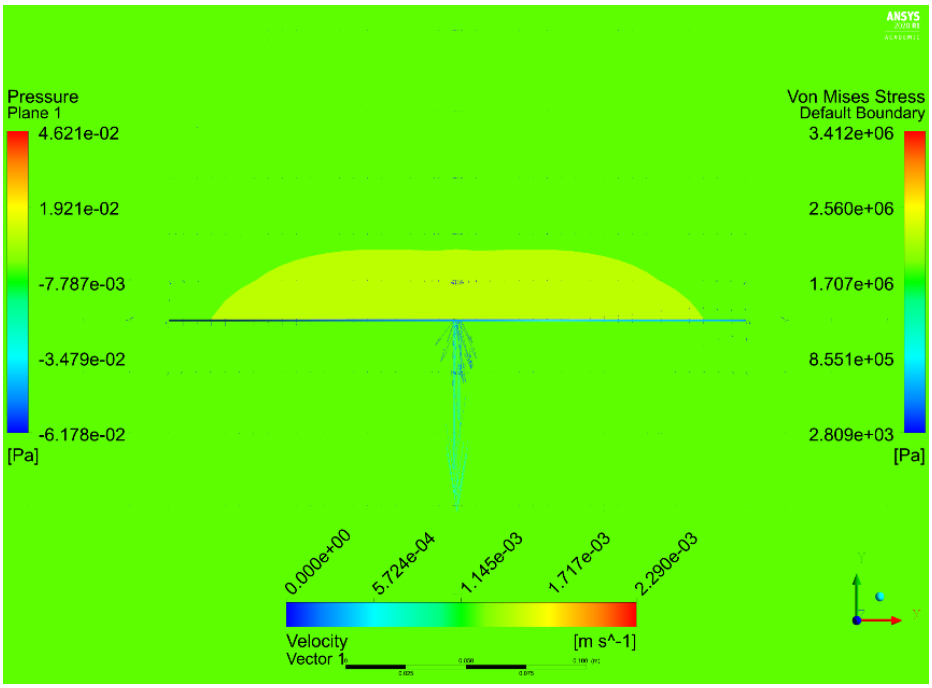

Figure 38. Frontal display of the graphical results at timestep 45 (t=4,5s)

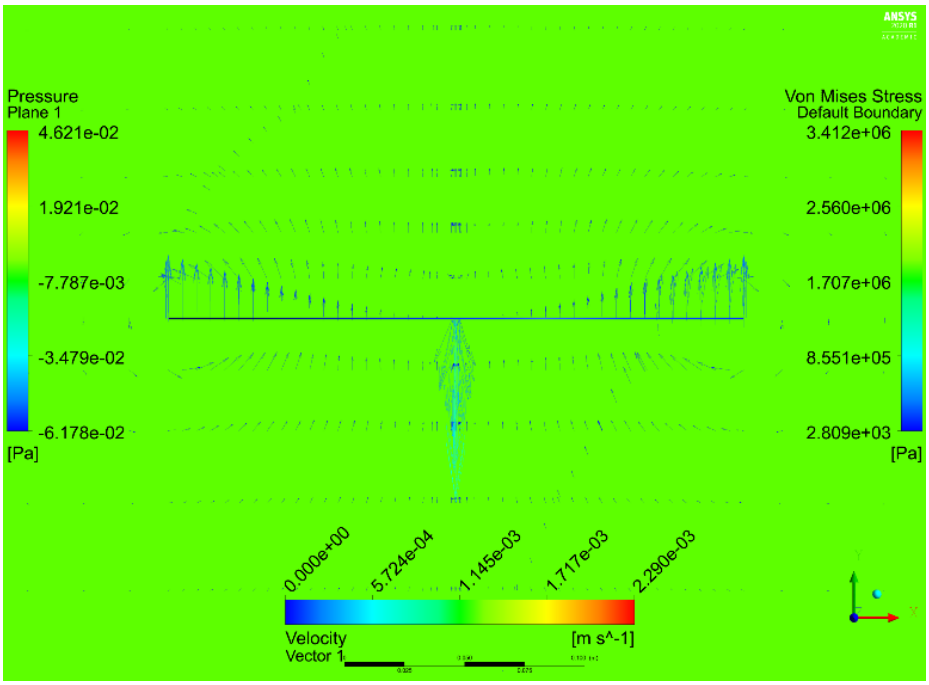

Figure 39. Frontal display of the graphical results at timestep 57 (t=5,7s)

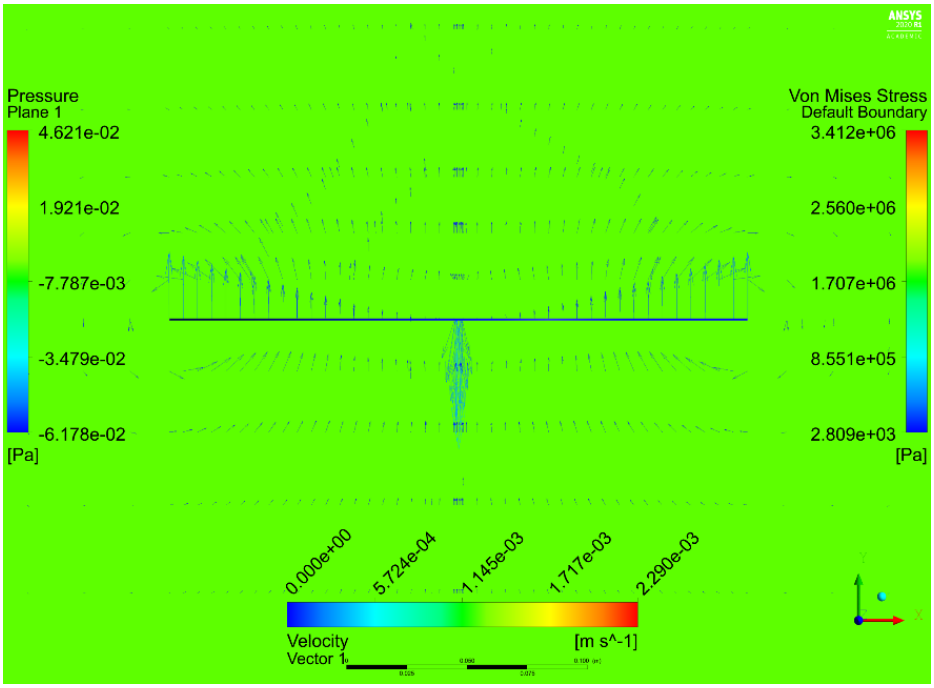

Figure 40. Frontal display of the graphical results at timestep 60 (t=6s)

9. Planning

The planning of the project is presented in the Gantt diagram of Figure 41 and the concrete day plan of all the tasks is shown in Table 15. The project has been divided in 9 tasks, starting from the 1st of April. The first month is spent on the detailed definition of the project and on the previous research that must be done on the topic. Also, the Ansys software must be correctly installed and the completion of a two-way coupled FSI Tutorial is high recommended before starting on the specific project's tasks. In addition, the tutorial would also serve as an introduction to the Ansys applications that would be used next.

The second month is basically spent on the model creation and meshing. Many difficulties may be encountered in the meshing process, so it might take more time than expected. Once the model is ready, modal analyses are performed to identify the modal properties of the model. Then, for the wall reduction analysis the geometry must be changed, but the modal properties are studied the same way as before. The fourth month is planned to perform the two-way coupled simulations. As many complications may appear and those simulations take a lot of time to complete, more time may be deserved. Until the date of submit, the report writing is carried out and finished.

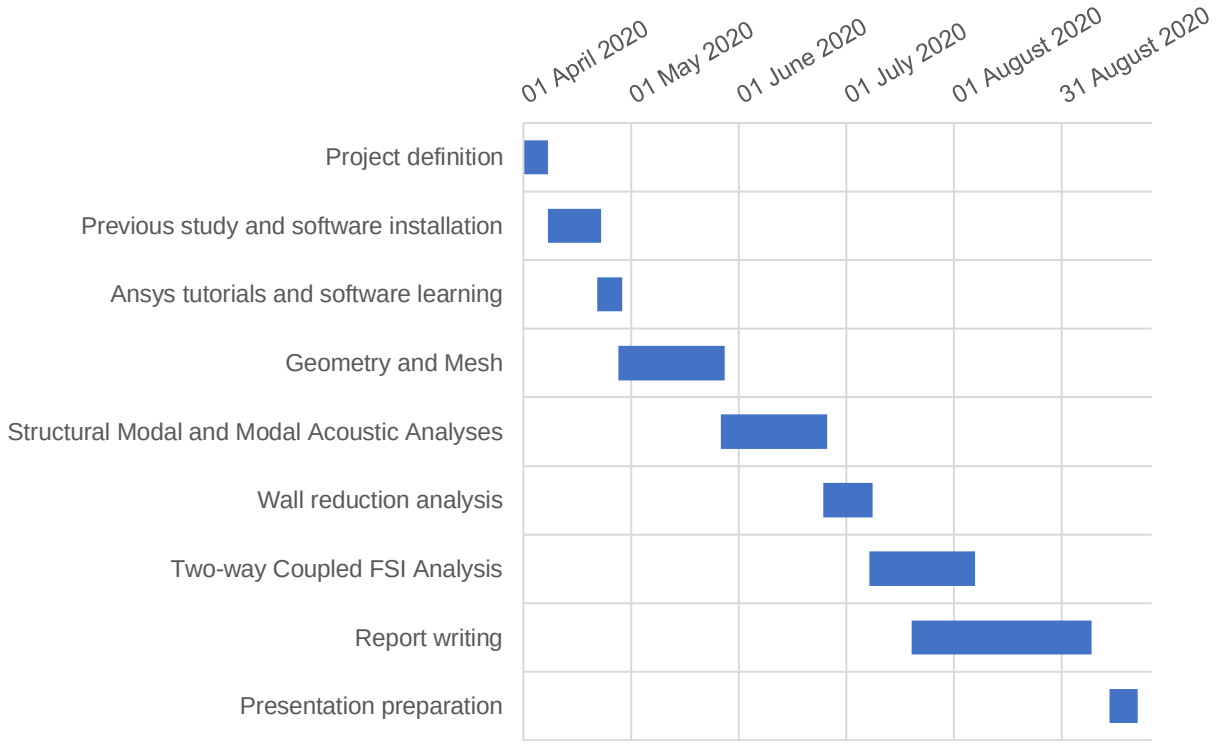

Figure 41. Planning of the project

TASK	START DATE	END DATE	DURATION
Project definition	01/04/2020	07/04/2020	7
Previous study and software installation	08/04/2020	22/04/2020	15
Ansys tutorials and software learning	22/04/2020	28/04/2020	7
Geometry and Mesh	28/04/2020	27/05/2020	30
Structural Modal and Modal Acoustic Analyses	27/05/2020	25/06/2020	30
Wall reduction analysis	25/06/2020	08/07/2020	14
Two-way Coupled FSI Analysis	08/07/2020	06/08/2020	30
Report writing	20/07/2020	08/09/2020	51
Presentation preparation	14/09/2020	21/09/2020	8
TOTAL			192

Table 15. Planning of the project tasks

10. Budget

Compared to other big scale projects, the costs of this project are considered low. In order to evaluate the magnitude of the total cost, it is been divided into personnel costs and infrastructure costs.

10.1. Personnel costs

Personnel costs refer to the labour value of staff that is working on the project. In this case, it concerns to the only the engineer that is in charge. The total project includes several tasks that require different effort from the engineer. Furthermore, depending on the knowledge of Ansys software, the engineer needs to pass previous stages to learn about numerical simulations.

Considering basic prior skills, the engineer is supposed to know how to use SpaceClaim or DesignModeler to build geometries. On the contrary, he will need to learn about modal acoustic analyses and two-way coupled simulations. Regarding to the latter ones, it is suitable to carry out a tutorial example to understand how the program works as many difficulties may appear otherwise. On another hand, the engineer may need to read about acoustics and modal properties to acquire expertise in the field. Also, he should be aware of previous investigations and research in the concrete area of study to understand the magnitude and the objectives of the current project.

Relative to the project's development, the engineer first needs to create the geometry and the mesh of the model. In this step, most of the time is spent in the meshing. Reaching an appropriate mesh may require the use of unknown meshing tools. Then, the completion of all the analyses depend on the type of simulation. In the modal analyses, the time is spent in changing the analysis settings and finding the desired results, as the solver doesn't need much time to converge. On the contrary, the two-way coupled simulations need many hours to complete, so the computational time comprises a big part of task. However, they need a deeper understanding and a more complicated setup.

Finally, the discussion of the results requires the total implication of the engineer, who has to extensively revise all the solutions obtained and evaluate the impacts. The redaction of the report is also included in this last stage.

10.2. Infrastructure costs

The infrastructure costs include the material needed for the engineer, the working space and the programs and software used for the development of the project.

The engineer must dispose a computer with a minimum RAM of 8 GB and an advisable i7 processor. The costs of the computer include maintenance and depreciation costs. Considering an annual use of 2000 hours, the maintenance cost has been evaluated as the 10% of the computer's value. For a 2000€ computer and a total of 370 hours applied in this project, maintenance costs are:

$$370\ hours \cdot \frac{0{,}1 \cdot 2000€}{2000\ hours} = 37€ \tag{20}$$

Taking into account that the computer has been used for 6 months around 5,5 days every week considering off days and holidays, the computer's use rises up to 132 days per year. Considering an annual use of 340 days every year during 3 years since the computer's purchase, depreciation costs are:

$$132\ days \cdot \frac{\frac{2000€}{3\ years}}{340\ days} = 258{,}82€ \tag{21}$$

Then, the total costs of the computer are:

$$37€ + 258{,}82€ = 295{,}82€ \tag{22}$$

Other material that the engineer might need is relative to office stationery, basically employed for sketches and notes.

A full Ansys license would be considerably desired, but the project can be also accomplished with a Student license. This last one is completely free, so it doesn't affect the costs. All the tasks concerning to the simulations and numerical computation can be done with the Student version of Ansys Workbench bundle, which include different applications. The engineer might use other programs to create geometries and edit post-processing results. Still, only Microsoft Word is indispensable for the report redaction although Microsoft Excel may be desirable for data manipulation. Considering the annual price of the basic Office licence and an Office employment of 60 days in this project, for a general 280 days use every year, the Microsoft Office costs are:

$$60\ days \cdot \frac{69€}{280\ days} = 14{,}79€ \tag{23}$$

Finally, the working space must be included. Considering that the rent price of a simple office is 200€/month, the cost for the whole project would be:

$$\frac{200€}{month} \cdot 6\ months = 1200€ \tag{24}$$

All the separate costs are indicated in Table 16, summing up to a total project cost of 12170,61€. Then, discounting an overhead of 6% and the VAT of 21%, the total budget of the project rises up to 15610,02€ (Table 17).

	Price	Hours	Cost
PERSONNEL COSTS			
Previous learning	20€/h	40	800€
Ansys simulations			
• Mesh	30€/h	70	2100€
• Modal simulations	25€/h	90	2250€
• Two-way coupled simulations	30€/h	90	2700€
Discussion and report redaction	35€/h	80	2800€
INFRASTRUCTURE COSTS			
Material			
Computer	2000€		295,82€
Office Stationery	10€		10€
Ansys Student	0€		0€
Microsoft Office	69€		14,79€
Working space	200€/month		1200€
TOTAL		370	**12170,61€**

Table 16. Total costs of the project with personnel and infrastructure costs

Total costs	12170,61€
Overhead (6%)	730,24€
Subtotal	12900,85€
VAT (21%)	2709,18€
TOTAL BUDGET	**15610,02€**

Table 17. Total Budget of the project

11. Environmental impact

The environmental impact of this project is low, since all the tasks have been numerically performed. Consequently, the only essential material has been one computer, which was already owned. As the computer had already been used and it was left available for future work, its manufacturing and residual impact has not been considered. What's more, no residuals have been produced at any moment of the project.

Therefore, the total environmental impact of this project is based on the electrical energy consumed by the computer. Considering a desktop power consumption of 170 kW per hour and a total of 370 hours of computer use, the total electricity consumed results in 62900 kWh. Considering that in Spain the CO_2 emission intensity due to electricity generation is 0,265 kg of CO_2/kWh [12], a total of 16668,5 kg of CO_2 have been emitted to the atmosphere.

Conclusions

Numerical analyses were conducted to determine the effects of water loading and fluid-structure interactions on the axisymmetric vibrations of a free circular Chladni plate. A structural-acoustic finite element model was built for structural modal and modal acoustic analyses, from which modal properties of the circular plate were studied. Concretely, the axisymmetric natural frequencies and the mode shapes were determined for the plate in vacuum, in air and fully submerged in water. While the first 6 axisymmetric natural frequencies were found in vacuum, only the first 2 and the first 4 were found in air and water, respectively.

Based on Leissa and Kwak's general equations for a free circular plate, numerical results were validated with theoretical results calculated with the model plate's properties. In the vacuum and air cases, a good agreement with the theory was found, with a maximum deviation of 0,7% in the natural frequency results. Higher differences were obtained for the plate in water, with a maximum deviation of 19,6%.

Due to the added mass effects of water, a significative frequency reduction was observed, with an average frequency reduction ratio of 66,7%. On another hand, all the mode shapes on water showed a significant decrease in the relative nodal circles, especially in the innermost compared to vacuum and air cases.

The effect of a wall boundary proximity was quantified comparing the axisymmetric natural frequency results of the plate in water at different wall distances. A clear frequency decrease was observed the more the distance between the plate and the wall was reduced. In wall distance ratios lower than 0,1, it was obtained that the highest the mode, the highest the frequency reduction ratio.

Finally, two-way coupled FSI transient simulations were achieved for a centre-fixed circular plate model. Fluid-structure interactions were concretely studied in the water model. Pressure, velocity and stress results were obtained for the coupled fluid-plate system, calculated at every 0,1 seconds of a total simulation time of 10 seconds. 2D Results were graphically visualized in the 3D coupled model and were compared at every timestep. Because of the small inner hole of the model plate, it was observed that a fluid flow slips through the hole according to the fluid mass conservation and distribution.

Bibliography

References

[1] Escaler, X., De La Torre, O., Axisymmetric vibrations of a circular Chladni plate in air and fully submerged in water (2018).

[2] Amabili, M., Pasqualini, A., Dalpiaz, G., 1995. Natural frequencies and modes of free-edge circular plates vibrating in vacuum or in contact with liquid. J. Sound Vib. 188 (5), 685–699.

[3] Amabili, M., Frosali, G., Kwak, M.K., 1996. Free vibrations of annular plates coupled with fluids. J. Sound Vib. 191 (5), 825–846.

[4] Amabili, M., 1996. Effect of finite fluid depth on the hydroelastic vibrations of circular and annular plates. J. Sound Vib. 193 (4), 909–925.

[5] Amabili, M., Kwak, M.K., 1996. Free vibration of circular plates coupled with liquids: revising the Lamb problem. J. Fluids Struct. 10 (7), 743–761.

[6] Askari, E., Jeong, K.H., Amabili, M., 2013. Hydroelastic vibration of circular plates immersed in a liquid-filled container with free surface. J. Sound Vib. 332, 3064–3085.

[7] Leissa, A.W., 1969. Vibration of plates, NASA SP (Scientific and Technical Information Division) 160.

[8] Kwak, M.K., Kim, K.C., 1991. Axisymmetric vibration of circular plates in contact with fluid. J. Sound Vib. 146 (3), 381–389.

[9] Kwak, M.K., 1991. Vibration of circular plates in contact with water. J. Appl. Mech. 58, 480–483.

[10] Kwak, M.K., Amabili, M., 1999. Hydroelastic vibration of free-edge annular plates. Trans. ASME. J. Vib. Acoust. 121 (1), 26–32.

[11] ANSYS System Coupling Tutorials, Release 18.2, August 2017.

[12] European Environment Agency, 2016, CO_2-emission intensity from electricity generation, *https://www.eea.europa.eu/.*

Additional literature

ANSYS Acoustics ACTx, Introduction to Acoustics, August 2017.

ANSYS Acoustics ACTx, Modal Analyses, August 2017.

ANSYS Acoustics ACTx, Harmonic Analyses, August 2017.

ANSYS Acoustics ACTx, Transient Analyses, August 2017.

Bourke, P., March 2003. Chladni Plate Mathematics 2D.

Bourke, P., April 2001, Chladni Plate Interference surfaces.

Kverno, D., Nolen, J., A study of Vibrating Plates.

The Experimental Nonlinear Physics Group, Chladni Patterns in Vibrated Plates. Department of Physics, University of Toronto.

Wang, C.Y., 2014. The vibration of concentrally supported free circular plates. J. Sound Vib. 333, 835-847.